PREPARATION OF NANOCRYSTALLINE COPPER OXIDE CATALYST FROM COPPER POWDERS

SAKOLLAPATH PITHAKRATANAYOTHIN

SUCHUTA NAKNAKA

EUMPORN BUAROD

A SPECIAL PROJECT SUBMITTED IN PARTIAL FULLFILLMENT

OF THE REQUIRMENT FOR THE DEGREE OF BACHLOR OF SCIENCE

IN PETROCHEMICAL TECHNOLOGY (INTERNATIONAL PROGRAMS)

FACULTY OF SCIENCE

KING MONGKUT'S INSTITUTE OF TECHNOLOGY LADKRABANG

ACADEMIC YEAR 2011

Title	Preparation of nanocrystalline copper oxide catalyst from copper powders	
Students	Mr. Sakollapat	Pithakratanayothin
	Ms. Suchuta	Naknaka
	Ms. Eumporn	Buarod
Degree	Bachelor of Science	
Major Program	Petrochemical Technology (International Program)	
Academic Year	2011	
Advisor	Asst. Prof. Dr. Pachernchaiyapat Chaiyasith	
Co-Advisor	Dr. Ruangdaj Tongsri	

ABSTRACT

CuO powders are well-known as a catalyst in many applications including gas sensor and thermoelectric materials, etc. It is widely used because of its high activity and selectivity in oxidation/reduction reactions. Nanometer-sized CuO particles are in interesting because of their high ratio of surface area to mass, which is expected to enhance catalytic performance of the material. The nanometer-sized CuO particles were prepared by two different routes. The first involved with reaction of pure Cu powders with nitric acid to form intermediate $Cu(NO_3)_2$ intermediate. In the second route, glacial acetic acid was employed to react with pure Cu powders to form $Cu(CH_3COO)_2$ intermediate. After purification, both intermediates were then reacted with NaOH via a solid-state route to form CuO powders. The intermediates and end product were characterized by using Fourier Transform Infrared Spectroscopy (FT-IR), scanning electron microscopy (SEM) and X-ray diffraction (XRD) technique. Experimental indicated that synthesis of the nanometer-sized CuO particles via the $Cu(NO_3)_2$ intermediate yielded slightly higher product output and fine particle sizes with larger aspect ratio. In contrast the $Cu(CH_3COO)_2$ intermediate route yielded lower product and fine particle sizes with smaller aspect ratio. However, due to extremely fine particle size it was observed that particle agglomeration could not be avoided particularly the CuO powders produced via the $Cu(CH_3COO)_2$ intermediate route.

Keywords: Nanocrystals, CuO, synthesis, characterization

Acknowledgement

We would like to thank our advisor, Asst. Prof. Dr. Pachernchaiyapat Chaiyasith and our co-advisor, Dr. Ruangdaj Tongsri for their supervisions in the experiments, helpful suggestions, skill coaching, encouragements and patience for our mistakes and doubtfulness. We also grateful to Dr. Pesak Rungrojchaipon and Dr. Samart Kongtaweelert for serving as the chairperson and the committee and valuable comments.

We gratefully acknowledge Mrs. Thanyaporn Yodkaew and technical staff in National Metal and Materials Technology Center (MTEC) for teaching and helping us to use XRD, SEM, TEM and FTIR, which made them a hard work from our project.

Sincere thank are due to the Faculty of Science, King Mongkut's Institute of Technology Ladkrabang and National Metal and Material Technology Center for support us in work place, equipments, chemicals and public utilities.

We would like to extend a sincere appreciation to all of professors, and friends for their support and encouragement. Especially, we dedicate the work to our family for their moral support. Lastly, we offer our regards and blessings to all of those who supported us in any respect during the completion of the project.

Sakollapath Pithakratanayothin

Suchuta Naknaka

Eumporn Buarod

Table of Contents

Table of Contents (con't)

List of Tables

List of Figures

List of Figures (con't)

Chapter 1

Introduction

1.1 Motivation

Tenorite or cupric oxide (CuO) is widely used as a catalyst due to its high activity and selectivity in oxidation and reduction reactions [1-3]. It can be used as a single catalyst, such as; for carbon monoxide oxidation [4] and for lactic acid production from glucose under hydrothermal conditions [5]. CuO can be used as a co-catalyst with various oxides for different applications. Co-catalysts of CuO with ZnO were used for methanol formation [3], for phenol oxidation in water [6] and for carbon monoxide oxidation [7]. Co-catalyst of CuO with AgO was employed for carbon monoxide oxidation [8]. Co-catalysts of CuO with CeO_2 were used for many applications including carbon monoxide oxidation [7, 9], volatile organic compounds (VOCs) oxidation [10], carbon monoxide removal [11] and water gas shift reaction ($CO + H_2O \longrightarrow CO_2 + H_2$) [12-14]. Co-catalysts of CuO with WO_3 were employed for organic substance photodegradation [15, 16]. Some complicated catalyst systems including $CuO/ZnO/Al_2O_3$ [17], $CuO/ZnO/Cr_2O_3$ [18], CuO, ZnO, Cr_2O_3/Al_2O_3 [19] and CuO/Cr_2O_3-Ga_2O_3 [20] were employed for water gas shift reaction. CuO is also applied in the forms of supported catalysts including zeorite encapsulated nanocrystalline CuO for oxidation of secondary alcohols [21], heterogeneous CuO/X zeorite for solar photocatalytic degradation of *o*-phehylenediamine [22], CuO/SnO_2 catalyst for H_2S gas sensors [23] and CuO/Al_2O_3 catalyst for selective NO-CO reaction [24].

CuO nano-particles are promising for many applications due to a large surface area per mass of the material. Various methods have been employed to produce CuO nanoparticles including one-step thermal decomposition [25], one-step hydrothermal method [26], one step solid state reaction [27], sol-gel method [28-31], sonochemical preparation [32], microwave radiation [33, 34], infrared irradiation [35], alkoxide-based synthesis [36], precipitation-pyrolysis [37], flame spray pyrolysis [38] and precipitation-stripping method [39]. Most of these methods suffer from material preparation difficulties due to complicated equipment sets, long times and high temperatures. A simple and efficient synthesis of CuO nanocrystals is obviously promising for industrial scale production. In this research, we are interested in

development of a simple route for producing CuO nanocrystals from water atomized Cu powders. It was reported that $Cu(NO_3)_2$ could be used as a starting materials to produce Cu(OH)2 nanowires, CuO nanowires and CuO nanobelts [40]. Thermal decomposition of $Cu(NO_3)_2 \cdot 3H_2O$ could yield CuO as a final product [41]. Experimental results showed that a hot aqueous solution of copper acetate, added with glacial acetic acid and NaOH could yield CuO nanocrystals [42] An ionic liquid assisted one-step low-temperature solid-state route using $Cu(CH_3COO)_2 \cdot H_2O$ as a starting material is a simple and efficient method for preparation of CuO nanocrystals [43]. From the literatures given above, it is possible for us to prepare CuO nanocrystals from Cu powders via two chemical precursors, such as $Cu(NO_3)_2 \cdot 3H_2O$ and $Cu(CH_3COO)_2 \cdot H_2O$. However, once these precursors have been prepared from Cu powders, a one solid-state reaction is then conducted to produce CuO nanocrystals. Chemical reactions for our approaches are as follows;

Synthesis via $Cu(NO_3)_2 \cdot 3H_2O$ intermediate;

$$Cu + 4HNO_3 \rightarrow Cu(NO_3)_2 + 2NO_2 + 2H_2O \quad (1)$$

$$Cu(NO_3)_2 + 2\,NaOH \rightarrow CuO + 2NaNO_3 + H_2O \quad (2)$$

Synthesis via $Cu(CH_3COO)_2 \cdot H_2O$ intermediate;

$$Cu + H_2O_2 + 2CH_3COOH \rightarrow Cu(CH_3COO)_2 + 2H_2O \quad (3)$$

$$Cu(CH_3COO)_2 + 2NaOH \rightarrow CuO + 2Na(CH_3COO) + H_2O \quad (4)$$

1.2 Objective

1. To investigate the effect of copper compounds prepared from copper powders on morphology of copper (II) oxide nanoparticles.
2. To prepare well-defined copper oxide nanoparticles, with narrow particle size distribution.
3. To compare the morphology of copper oxide that prepared from different copper compounds.

1.3 Scope

1. For preparation of copper (II) oxide nanoparticles
   A. Cu powders are used as starting materials.
   B. Copper nitrate & Copper acetate and NaOH are used as reactants.
2. For characterization of copper (II) oxide nanoparticles, the XRD, FTIR, SEM and TEM were used.

1.4 Expected results

To obtain suitable condition of the solid-solid reaction for prepared a well-defined copper (II) oxide nanoparticle.

Chapter 2

Literature Review

2.1 Copper (II) oxide

2.1.1 Properties

Copper oxide is formed when copper is exposed to oxygen and oxidizes. There are two types of copper oxide: copper (I) oxide and copper (II) oxide. Copper (I) oxide is referred to as cuprous oxide, while copper (II) oxide is known as cupric oxide. Both are used as pigments and semiconductors. Even though they have the same components, but each of them has slightly different characteristics.

Cupric oxide (CuO) is a black material. It is a p-type semiconductor with a narrow band gap which shows the interesting electrochemical and catalytic property. CuO has received considerable due to its application in many fields. This copper oxide is used as pigment in clay glazes. Several colors, including red, blue and green can be derived from it. It is also used to produce cuprammonium hydroxide, a material that used to make rayon. Exposure to this type of copper oxide can also be dangerous. If inhaled, cupric oxide can cause irritation to the lungs. It can also cause metal fume fever.

The copper atom is coordinated by 4 oxygen atoms in an approximately square planar configuration.

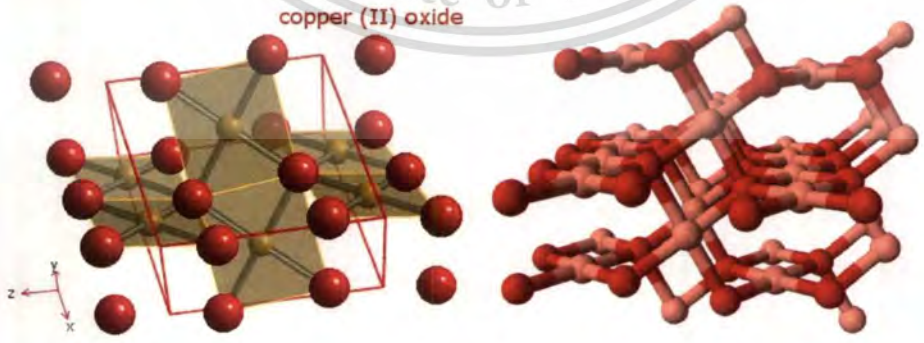

Figure 2.1 A structure of Copper (II) oxide [44,45]

Table 2.1 The Physical and chemical characteristic of Copper (II) oxide

Molecular formula	CuO
Synonyms	Banacobru OL; C.I. Pigment Black 15; Chrome Brown; Copper monoxide; Copper oxide(CuO); Copperoxide (CuO); CuO; Precipitated cupric oxide; Cupric oxide
Molar mass	79.545 g/mol
Appearance	Black to brownish - black Powder, granules or wire
Density	6.31 g/cm ^{3}
Odor	Odorless
Melting point	1201 $^{\circ}$C (1474 K)
Boiling point	2000 $^{\circ}$C
Solubility in water	Insoluble
Solubility in Ammonium hydroxide	Soluble
Solubility in mineral acid	Hydrochloric acid, Sulfuric acid Nitric acid
% Volatiles by volume @ 21 $^{\circ}$C	0

Nanoparticles are sized between 1 and 100 nanometers. Nanoparticles may or may not exhibit size-related properties that differ significantly from those observed in fine particles or bulk materials. Nanoparticle research is currently an area of intense scientific research, due to a wide variety of potential applications in biomedical, optical and electronic fields. Nanoparticles are great scientific interest as they are effectively a bridge between bulk materials and atomic or molecular structures so the nano-scale exhibit a number of special properties compared to bulk material.

Nanoparticles have a very high surface area to volume ratio, increase special activity, special electronic properties and unique optical properties. This provides a tremendous driving force for diffusion,

especially at elevated temperatures. Sintering can take place at lower temperatures, over shorter time scales than larger particles.

At a small end of size range, nanoparticles are often referred to as clusters. Nanospheres, nanorod, nanofibers and nanocups are just a few of shapes that have been grown.

Characterization is done by using a variety of different technique, mainly drawn from material science. Common technique are electron microscopy (TEM, SEM) atomic force microscopy (AFM), dynamic light scattering (DLS), x-ray photoelectron spectroscopy (XPS) and powder x-ray diffraction (XRD).

2.2 Copper (II) Oxide Nanoparticles

The higher oxide of copper, CuO is known as tenorite. It is a black solid with an ironic structure which is semiconductor nanocrystals. CuO nanoparticles have attracted much attention in recent years because their optical properties can be significantly different from those of their bulk counterparts and it is the basis of several high-T_c superconductors. CuO nanoparticles have been prepared by nanochemical method, sol-gel technique, one-step solid-solid reaction method at room temperature, electrochemical method, thermal decomposition of precursor, and so on.

Copper (II) oxide belongs to the monoclinic crystal system, which a crystallographic point group of 2/m or C_{2h}. The space group of its unit cell is C_2/c, and its lattice parameters are

a = 4.6837(5),	$\alpha = 90^\circ$
b = 3.4226(5),	$\beta = 99.54^\circ$
c = 5.1288(6),	$\gamma = 90^\circ$

The type of crystal structure can be divided into different categories which have different characteristics. Each type has a different description.

1. Copper (II) Oxide (CuO) nanodots or nanopowders are white spherical high surface area metal particles. Nanoscale Copper (II) Oxide particles are typically 1-30 nanometers (nm) with specific surface area (SSA) in the 100-200 m^2 /g range. [46, 44]

2. Copper (II) Oxide (CuO) nanorods are synthesized by annealing a copper foil. Annealing of copper foil leads to the formation of CuO nanorods spread in a large area by annealing a copper foil. Annealing of copper foil leads to the formation of CuO nanorods spread in a large area. In order to study the effect of oxygen flow rate on the growth of nanorods the different samples were prepared by annealing at 500°C in 35, 150, 300 and 500 ml/min of oxygen flow. Annealing of foil was also carried out in air to know the effect of a mixture of gases on the growth of CuO nanorods. [47, 48]

Figure 2.2 HRTEM image of CuO nanorods obtained after hydrothermal treatment [49]

3. Copper (II) Oxide (CuO) nanowire has been prepared by an oxidation reaction. A copper plate was heated at 400-600°C in a furnace tube under a normal atmosphere. After heating, the color of the copper plate turned black. It was found that the black products were the CuO which exhibited nanostructure with a diameter ranging from 100-300 nm. The diameters of CuO nanowires was about 100 nm at the heating temperature of 400°C and about 200-300 nm at 500-600°C. [50, 51, 52]

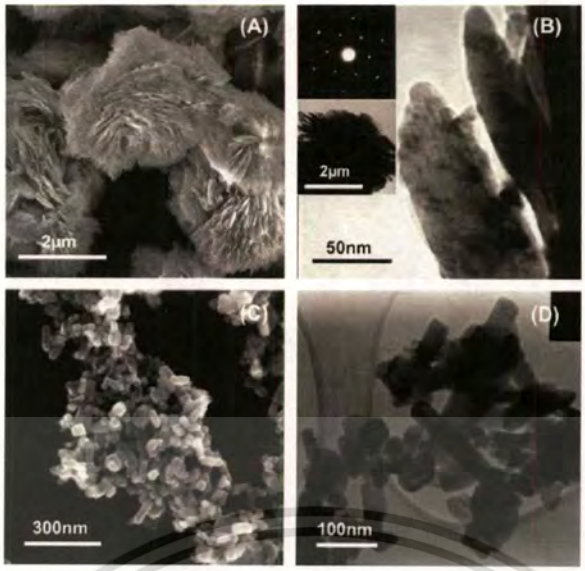

Figure 2.3 (A) FE-SEM images of CuO nanowires and (B) TEM image of CuO synthesized by the CHM method. (C) FE-SEM image and (D) TEM image of CuO synthesized by the CMS method [53]

4. Copper (II) Oxide (CuO) nanoplate

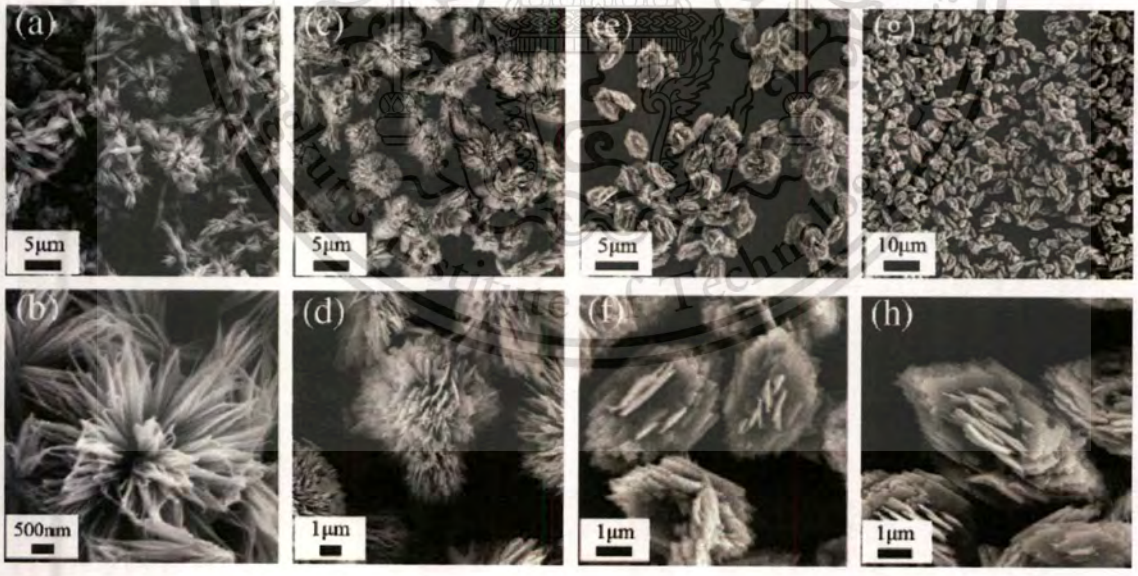

Figure 2.4 SEM images of CuO nanoplates [54]

5. Copper (II) Oxide (CuO) nanopindle

Figure 2.5 TEM images of CuO nanopindle [55]

Three different nanostructure of CuO (wires, platelets, and spindles) have been synthesized by thermal annealing of copper thin films deposited onto silicon substrate. The order of the electron transfer ability about the three nanostructures is: CuO nanospindles > CuO nanowires > nanoplatelets.

2.2.1 Application of Copper (II) Oxide nanoparticles

2.2.1.1 Electronic and optoelectronic devices

1. Conductive ceramics

The research about CuO ceramics itself is little and as a result, the knowledge of electric properties and crystalline analyses are not clarified yet. Recently, the authors have found out that alkaline or alkaline earth oxides act as the sintering aid of CuO ceramics and show good linearity of their resistivity at high applied field. A new type or high performance ceramic resistor will be developed for the

component equipments in fields of generation and delivery power systems. For example; transformers, circuit breakers and arrestors.

Conductive ceramics have been heretofore widely utilized as an electrode and a heat emitter according to superior stability against corrosion and thermal degradation of ceramics. It is quite useful material for an electrode. Since it consumes less amount of electric power and has excellent corrosion stability. Conductive ceramics have also applied to an electrode of various sensors to convert some atmospheric change to an electrical signal.

Furthermore, application of conductive ceramics includes uses ceramics for a transparent electrode ceramics for an optical switch and optical shutter. In considering thermal resistance of ceramics can be very useful for a heat emitter of a furnace or an electrode of a fuel cell.

As described above, conductive ceramics have been used in various fields of industries. Accordingly, conductive ceramics are desired which can be produced easily and economically using easily obtainable materials.

A process for producing conductive copper oxide ceramics of $(M_xCu_y)_7O_z(NO_3)$ where in M is represents at least one element selected from the group consisting of In, Sc, Y, TI and Ga which x+y is a value of 1. x/y is a number of from 0 to 10 and z is a number of from 6 to 8, which process comprises mixing at least one nitrate of a metal selected from the group consisting of In, Sc, Y, TI and Ga, with copper nitrate and firing the mixture at from 200°C to 600°C.

2. Gas sensors

Copper (II) oxide is a semiconductor that important to adopt a gas sensor. Using principles of changes electrical resistance, the characteristics of sensor were observed from the changing of resistance in air and in gas sample at work temperature of 150 – 250 °C. It was found that the sensor resistivity under the gas sample atmosphere is lower than the resistivity in air.

The thin films of copper (II) oxide were deposited using a reactive DC sputtering method for gas sensor applications. Supported copper (II) oxide nanosystems were on Al_2O_3 substrates. Gas sensing

performances in the detection of Volatile Organic Compounds (VOCs; e.g. CH_3COCH_3, CH_3CH_2OH) revealed appreciable responses even at moderate temperatures, with characteristics directly dependent on the system composition and nano-organization.

3. Superconductor

Superconductivity is a phase of matter. The graph below shows where phase changes occur in high-temperature copper oxide superconductors. Depending on the temperature (in Kelvin) and the number of electrons in its crystal structure. (Holes are the plates left when atoms in the surrounding crystal matrix pull electrons away. Holes are like electron because they can move around and carry charge in conductors or superconductors). Superconductivity occurs in the half-circle region at the bottom, when the material has from 5 to 25 present holes and the temperature is below about 130 K. At low-electron hole concentrations, the material becomes an insulator, while at high concentration it is a conventional metal – a good electrical and heat conductor. Remarkably, by changing electron concentration only 5 percent, the material goes from a perfect insulator (incapable of transporting any electricity) to the strongest known superconductor (a perfect conductor of electricity).

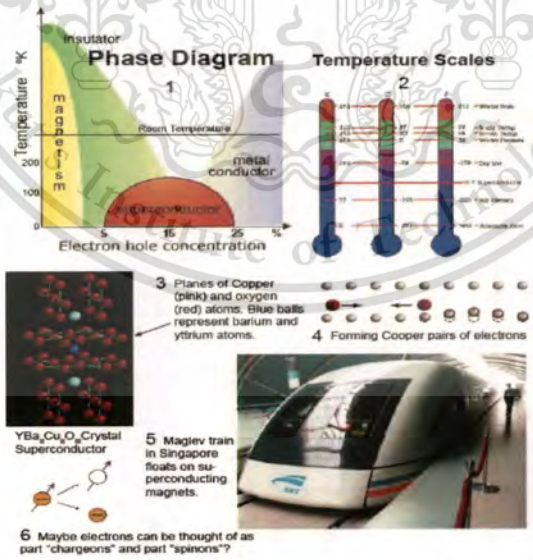

Figure 2.6 Phase change occur in high-temperature copper oxide superconductors [56]

4. Optical switches, shutters

An electrically controlled optical switch employs an electro-optical crystal of the kind exhibiting birefringence in each of two different light paths when the crystal is disposed in orthogonally oriented electric fields, with each light path being sensitive to a different one of the two electric fields and each path having its own set of fast and slow axes. A crystal of copper oxide has those properties. Electrodes are provided for separately establishing each of the two electric fields and control circuitry allows only one field at a time to be established. Polarizes are situated at opposite end of the electro-optical crystal in alignment with each of the two paths. Adjacent one end of the crystal are disposed a beam splitter and a right angle prism. The prism is arranged to receive some of the beam splitter and reflect that light along one of the paths of the crystal while another portion of the entering light proceeds through the beam splitter into the other path of the crystal. The Polarizer blocks the light in one path while enabling light to emerge from the other path.

5. Magnetic storage media

Materials that combine coupled electric and magnetic dipole order are termed "magneto electric multiferroics". In the past few years, a new class of such material "induced-multiferroics" has been discovered, e.g. Copper oxide wherein non-collinear spiral magnetic order breaks inversion symmetry, thus inducing ferroelectricity. Here, we propose that Copper (II) oxide (containing Cu^{2+} ions) having large magnetic super exchange interactions can be good candidates for induced - multiferroics with high Curie temperature (TC).

6. Dry cell batteries (solar cell) and copper salt production

Copper (II) oxide can be used to produce dry cell batteries. It has also been used in wet cell batteries as the cathode, with lithium as an anode, and dioxalane mixed with lithium per chlorate as the electrolyte. Copper (II) oxide is a basic oxide, so it dissolves in material acids such as hydrochloric acid, sulfuric acid or nitric acid to give the corresponding copper (II) salts;

$$CuO + 2\,HNO_3 \longrightarrow Cu(NO_3)_2 + H_2O \qquad (2.1)$$

$$CuO + 2\,HCl \longrightarrow CuCl_2 + H_2O \qquad (2.2)$$

$$CuO + H_2SO_4 \longrightarrow CuSO_4 + H_2O \qquad (2.3)$$

It can also be reduced to copper metal using hydrogen or carbon monoxide:

$$CuO + H_2 \longrightarrow Cu + H_2O \qquad (2.4)$$

$$CuO + CO \longrightarrow Cu + H_2O \qquad (2.5)$$

7. Organic catalyst

Copper (II) oxide has also been exploited as a powerfully heterogeneous catalyst to convert hydrocarbons completely into carbon dioxide and water. CuO based catalysts (several kind of support, including metal oxides, zeolites, mesoporous silica, carbons and so on) have been extensively examined as a possible substitute for noble metal catalysts, because they have much lower cost and comparable or even higher activity for CO oxidation.

2.2.1.2 Pigment for glass manufacturer blue, red and green colors in the glass

1. Copper oxide can be added to produce green colors in the glass

If the glass was made of pure silica, the observe color is colorless or look pale green but purifying is so difficult so CuO is a choice for reduce the production cost.

Copper–containing glazed glasses in the B_2O_5-SiO_2-Al_2O_3-CaO-CuO system with a copper oxide molar content of 5 to 25%, added during synthesis of the glasses, were investigated. The glasses with a minimum content of 15% B_2O and 15-20% CuO crystallized during processing with separation of fine-needle CuO crystals. However, all glasses formed a good glaze coating when applied on ceramics at temperature of 900-1000°C. The CuO crystals totally dissolved in the melt.

2. Coating (antifouling agent encapsulating agents).

A Copper (II) oxide based antifouling has highly active from an electrolysis standpoint and more costly due to the larger quantities of 50 active ingredients needed. It is an agent that inhibits the growth of barnacles and other marine organisms on a ship's bottom (an antifouling paint or other coating). Copper (II) oxide compounds have been the most often used agents in this application since they are effective against both soft and hard fouling organisms. However, in spite of their performance, they have a negative impact on the marine environment and their long half in the environment has prompted marine paint manufacturers to look for a non persistent alternative.

A process for encapsulation is provided. Generally, the material involved are those which tend to lose at least part of their original properties upon exposure to auto-oxidative, thermal, or humid conditions. The process comprises constituting the material to be encapsulated in or as a viscid medium and dispersing the medium as particulates into an atmosphere containing an agitated quantity of a powdered, sorbent, film-forming agent. The dispersed particulates must have a tacky surface. The powdered agent adheres to this tacky surface and absorbs sufficient liquid to gel the coated particulates and to form a continuous, substantially non-crackable and dry encapsulating film around each of the particulates.

3. Making fibers (rayon).

Impregnation or coating of cotton and polyester fibers with cationic copper endows them with potent broad-spectrum antibacterial, antiviral, antifungal, and antimite properties. This durable platform technology enables the mass production of woven and non-woven fabrics, such as sheets, pillow covers, gowns, socks, air filters, mattress covers, carpets, etc. without the need of altering any industrial procedures or machinery, but only the introduction of copper oxide-treated fibers. The biocidal properties of fabrics containing 3-10% copper-impregnated fibers are permanent, are not affected by extreme washing condition, and do not interfere with the manipulation of the final products (e.g., color, press, etc.). In this article, the authors describe data showing that (i) antifungal socks containing 10% w/w (weight/weight) copper-impregnated fibers alleviate athlete's foot; (ii) antimicrobial fabrics (sheets)

containing 10% (w/w) copper-impregnated fibers decrease bacterial colonization in a clinical setting; and (iii) these products do not have skin-sensitizing properties or any other adverse effects. Taken together, these results demonstrated the wide preventive and curative potential of copper oxide-impregnated apparel products.

2.2.2 Preparation method of CuO nanoparticles

2.2.2.1 Solid-Solid reaction

A solid-solid reaction, also called a dry media reaction or a solvent less reaction, is a chemical reaction in which solvents are not used. In a normal reaction, the reacting agents, also called the reactants, are placed in a solvent before the reaction can take place. These reactants react to form a new substance. After the reaction is completed, the new products are removed from the solvent. A solid-solid reaction, however, allows the reactants to chemically react without the presence of a solvent.

The advantages of solid-solid reaction ripple throughout many industries. It is important to economics because the elimination of solvents mean that products will cost less. This will make those products cheaper to buy. Producing materials from a solid-solid reaction will mean that product is able to bypass the purification process.

The chemical equation which showed the preparation of Copper oxide by used copper powder as a starting material. With it will produce copper nitrate and copper acetate as intermediate. And we used both of them to produce Copper oxide.

$$Cu + 4HNO_3 \longrightarrow Cu(NO_3)_2 + 2H_2O + 2NO_2 \quad (2.6)$$

$$Cu(NO_3)_2\,(s) + 2NaOH\,(s) \longrightarrow Cu(OH)_2 + NaNO_3 \quad (2.7)$$

$$Cu + 2CH_3COOH + H_2O_2 \longrightarrow Cu(CH_3COO)_2 + H_2O \quad (2.8)$$

$$Cu(CH_3COO)_2\,(s) + 2NaOH\,(s) \longrightarrow Cu(OH)_2 + 2CH_3COONa \quad (2.9)$$

$$Cu(OH)_2 \longrightarrow CuO + H_20 \quad (2.10)$$

There are various methods for synthesis of nanoparticles. In the two decades, the CuO have been studied in a nano scale. There are many methods has been developed to achieve the definite size and shape. Chen et al. [57] produced Cu and CuO nanomaterials from inverse micelle solutions. A latter year, many researches had reported incessantly, Kumar et al. [47] prepared a stable colloidal solution of copper (II) oxide 6 nm in octane by an inter phase synthesis at interaction of copper (II) oleate and sodium hydroxide is solved in octane and water, respectively. He said that method was too elaborate and not suitable for preparation of CuO nanoparticles in large amounts.

In the 1998 the solid-solid reaction under ambient condition was discussed by D.Chen, G.Shen, K.Tang [57], they presented a single-phase CuO with monoclinic structure with an average size of 12 nm were obtained but it was stable due to grains grow with time, which can be manifested by both XRD and Raman spectroscopy. None of research studies further for this method. In next year the metal-organic decomposition technique was applied to synthesis the CuO in polypyrole and D. Chen et al. [57] reported copper (II) oxide sols of definite size and shape in aqueous solutions. In addition in 1999, the direct deposition method allowed the precipitation of the tenotite copper (II) oxide in large amounts. However it was too difficult to control the grind size of the resulting copper (II) oxide.

A. K. Srivastava et al. [47, 48 and 59] developed a novel sonochemical method. This method has been successfully to synthesis the CuO nanoparticles in various organic solvent such as DMF. Using copper acetate as starting material, this method only affords the formation of CuO in a very low yield. Moreover in the same year he tried to develop new sonochemical method to prepare in a high yield but need expensive ultrasonic equipment with severe condition of reaction and excessive organic solvents. He continued the preparation of high purity nanocryatlline CuO in the next year.

Zhong-shan Hong and Yong Cao, Ying-fa Deng [60] reported successfully novel alcoholthermal process using copper acetate as starting material at mild conditions to achieve a stable CuO nanoparticle of 3-9 nm with a yield of as high as 100% at 110°C. The result was investigated by TEM, XPS and XRD. Hong et al. [61] reported the preparation of nanosized CuO by alcohothermal route, but the organic solvent in large amount were required in the preparation process, in 2002

Wang et al. [62] have been successfully prepared CuO nanoparticles with an average size of 4 nm. Using Copper (II) acetate and sodium hydroxide as the starting material and absolute ethanol as solvent. PEG was used to prevent the CuO nanoparticles agglomeration of over 200 nm. This method produced with regular shape, small size, narrow size distribution and high purity. But it was failed to obtain pure single phase of CuO. The products obtained were mixtures of monoclinic CuO and some other unknown products. Xia and co-workers [63] produced CuO nanowise but required the severe reaction aonditions and heat treatment over 500 °C

A. K. srivastava prepared the CuO nanorod which is a one state that has been studied. A copper foil were annealed that leaded to the information of CuO nanorods spread in a large area. It was found that under the same conditions of growth gave nanorods of similar diameter and length so indicate that this method is reproducible. D. Chen and coworker [57] prepared a unique shuttle-like morphology nanocrystals have been obtained via a simple and convenient hydrothermal decomposition route by $CuCl_2.H_2O$ and NaOH were used as starting materials. The product was characterize by XRD, TEM, Raman spectra and XPS which found the CuO crystal have regular shape, uniform size distribution with high yield. It was reported that with the increasing the reaction time, the shuttle-like CuO crystals may further grow into flower-like crystals.

J. Zhu et al. [59] developed a successfully novel quick-precipitation method for the preparation of 6 nm of highly dispersed CuO nanoparticles and narrow particle size diatribution, which shown in the TEM image, using copper acetate aqueous solution and sodium hydroxide as starting materials. It was reported that spherical, ellipsoidal and needle shaped CuO nanocrystals can be obtained by varying there action conditions, temperature. The differences of shape represent the surface area of CuO particle which play an important role for its application. That was very interesting at that time. XRD presented no peak of impurity. The UV-Visible absorption spectra were used to investigate the dispersion. Needle-shaped nanocrystalline CuO was prepared continuously by liquid hydrolysis of $Cu(OAc)_2$ [63]. The result was showed that the diameters of the needle-shaped CuO nanocrystals can be controlled between 10 and 45 nm simply by varying the concentration of $Cu(OAc)_2$ solution, the presence of small amounts of cetyltrimethylammonium bromide (CTAB) can render needle-shaped CuO well dispersed.

G.H.Du, G.Van Tendeloo [64] discussed the growth mechanism of nanostructures via one dimensional nanostructure because of the most active area. CuO nanowires were prepared by self-assembly of nanocrysals with a size of 4x9 nm. No organic template and catalyst are needed and the method is suited for large-scale preparation. The microstructures of these nanoscale products are analyzed in detail using transmission electron microscopy (TEM), which allows proposing a formation mechanism. These nanocryarals tend to orient their (110) axis parallel to the growth direction. The diameter of CuO nanowires are in the range from 5-20 nm and their length varies from 500 nm to 2 um. The CuO nanobelts are single crystalline and lie on the (001) plane with the edge surfaces as the (110) crystal plane; the growth direction is the (010) direction. F. Teng et al. [65] have reported the self-organization of CuO hierarchical microspheres.

Manmeet et al. [66] have been synthesized CuO nanowires by thermal oxidation of copper foils in oxygen atmosphere. The branching of nanowires has been expected to further improve their gas sensing and catalytic properties due to increase in surface-to-volume ratio. Morphology and microstructure of the nanowires was studied as a function of temperature and annealing time using scanning electron microscopy, energy dispersive x-ray analysis, x-ray diffractograms, x-ray photoelectron spectroscopy, transmission electron microscopy and selected area electron diffraction. Nanowires were found to grow perpendicular to the surface of copper foil preferentially along (101) direction. The length of nanowires was maximized by increase with annealing time and for long times branched structure was observed. A "blue-shift" in comparison to bulk CuO was observed in the band gap as determined from optical absorption spectra. For this method, it provides simple, convenient and fast method.

T.Ahmad et al. [67] revealed the reverse-micellar route to synthesis copper oxide nanoparticles of 25-30 nm size with minimal agglomeration by water-in oil microemulsions with two different a polar solvent (isooctane and n-octane). The samples studied was shown that the grain size was highly dependent on the nature of non-polar solvent, 25-30 and 80-90 nm sized nanoparticles with isooctane and n-octane, respectively. The Neel temperature of CuO nanoparticles obtained from isooctane was abount 80K. For the larger particles obtained from n-octane, the transition temperature shifted to higher temperature (220 K) near that of the bulk. It can be said that the mature of the oil phase affected the size of the

nanoparticles, since they obtain much larger (80-90 nm.) particles using the straight chain hydrocarbon (n-octane). The onset temperature of weak ferromagnetism was size-dependent and decrease with size, although the short-range antiferromagnetic correlations appear unaffected.

L.Sun et al. [68] reported that aggregation of CuO nanoparticles was supposed to be made through the adsorbed NH_3 molecules. The liquid ammonia can be used as primary material being synthesis the CuO nanoparticles. TEM image indicated that the size of CuO nanoparticles were in the range of 5-10 nm, but aggregation could not be avoided.

J. Pike et al. [58] studied CuO nanoparticles dispersion in non polar media with no dispersant added or using oleic acid as the dispersing agent, respectively. M. Guedes et al. [69] studied CuO nanoparticles dispersion in water with no addition of dispersing agents. Djinovic et al. [14] prepared CuO/CuO composite hallow microspheres with controlled diameter and composition. S.wang et al. [70] fabricated CuO nanoparticles interlinked microspheres cages by solution method. They reported the synthesis of CuO with the tetrahedral nanocage morphology by the oxidation of alpha-CuI nanotetrahedrons. This method concentrated in the crystalline structure.

Dong Yan Han et al. [71] have improved the reversed micelles via microemulsion method. They described new water-in-oil reverse micelles used to prepare CuO nanoparticles, i.e. TritonX-100 / (n-hexanol + n-pentanol) / cyclohexane / water micro emulsion system. It was presented pseudoternary phase diagram. The size, shape and size distribution of CuO nanoparticles were strongly affected by molar ratio of water to surfactant. The morphology features of the nanoperticles investigated by TEM show that the particles with a spherical shape at lower water content were monodispersion with minimal agglomeration. With water content increasing, the particles size become larger and took different shape. Usefully, being route to the synthesis of metal oxides with different morphologies and size distributions. However, little work has been published concerning the preparation of CuO nanoparticles by means of the microemulsion method in literatures.

Recently, nanostructures of semiconductors have caught attention due to the unique property of having a huge surface-to-volume ratio which was expected to enhance the performance of the devices

based on semiconductor nanostructure. An oxidation reaction is one of the more practical and simple ways of synthesis. P. Pak et al. [50] have published their research in 2008 the oxidation reaction of copper plate has been revealed to prepare the CuO nanowires using various ethanol concentration. They studied the CuO nanowires gas sensing properties. It was found that from FE-SEM, EDS and TEM characterization, CuO nanowires exhibited diameters of 100-400 nm having a monoclinic structure with a growth along (110) direction. Moreover, the CuO nanowires sensor responded to ethanol vapor, exhibiting the optimum sensitivity of 1.5 to an ethanol vapor concentration of 1000 ppm with a working temperature of 240 °C, the response time of 110 s and recovery time of 120 s. The CuO nanowires could be explored for gas sensor application.

CuO nanostructures have been also synthesized in ionic liquid [72]. It was assisted one-step, low-temperature solid-state route. This is a new synthetic alternative to synthesize nanomaterials with specific alternative such as convenience, economical, less energy, material consumption and high yield. Besides, J.W Zhu and coworker prepared CuO bulk and CuO film [73] with network like structure and negative electrodes was applied on lithium ion batteries. However, there were almost no reports about the application of CuO on capacitors by.

H. Zhang et al. [73] synthesized a flower-like CuO by a simple chemical precipitation method at low temperature 80°C. As above this shape has been found coincidentally by D. Chen and coworker in 2003. They found that flower-like CuO had a higher specific capacitance and excellent cycle performance. The electrochemical property of copper oxide could be enhanced greatly by the improving of morphology. The morphology of CuO nanocrystals can be influenced by category of alkali. The specific capacitance of flower-like CuO is higher than CuO sheet and globular CuO. The attained value demonstrates that CuO have an ideal capacitance property and low-cost CuO is a potential electrode material in capacitor. The XRD patterns showed the monoclinic CuO phase with lattice constants. No obvious peak of impurity was found.

M.A.Dar et al. [74] revealed the CuO nanoneedles synthesized by hydrothermal method. It presented the formation of high-density CuO nanoneedles with ultrathin nanotip at low temperature. The CuO nanoneedles have monoclinic structure with single crystalline phase. It revealed a ferromagnetic

behavior of the CuO nanoneedles. Next few days, 25th June 2008 Microwave-hydrothermal methods, by F. Teng et al. [65] have also been employed to control the morphologies of these oxides. This reported an effective method to obtain the desirable crystal such as controllable morphology, low aggregation and high crystallinity. In this work, the flower-like CuO nanostructure was hydrothermally synthesized using copper threats as precursor without using any template.

A highly pure, well-dispersed, 10-nm CuO nanoparticles were obtained [75] by a hydrothermal reduction process, with oxalic acid as precipitator. The CuO nanoparticles were characterized by x-ray powder diffraction, field-emission scanning electron microscopy, and high-resolution transmission electron microscopy. The CuO nanoparticles were modified onto a gold electron to study the effect on the redox of the rutin. Cyclic voltammetry results showed that the CuO nanoparticles were very active for rutin and that the CuO-nanoparticle-modified electron can even determine in a certain range of concentration from 5.0 10-7 to 5.0 10-4 mol L-1 by differential pulse voltammertry, which provides a new application for CuO nanoparticles.

S. Wang et al. [70] reported CuO have been successfully fabricated through a simple hydrothermal method in the presence of cetyltrimethylammonium bromide (CTAB) as the template. Urea was used as a good precipitating agent. The dandelion-like CuO hollow microspheres was prepared and exhibited a high photocatalytic activity for the photocatalytic decolorization of RhB aqueous solution under UV-light illumination. The SEM image of the dandelion-like CuO hollow microspheres was obtained by hydrothermal reaction for 6 h. The reaction temperature, surfactant nature and the molar ratio of Urea/Cu (II) all are crucial roles on the formation of the hierarchical CuO hollow microspheres; otherwise no hollow microspheres could be formed. The unique applications are areas such as catalysis, electronics, filters, coating, and encapsulating agents due to their low density, large specific area and interesting optical properties. Back to 2006 S. Wang et al. [70] fabricated hollow CuO microspheres on a large scale through a rational complexing reagent-assisted approach at low-temperature. For the new one colloidal cupric oxide (CuO) nanoparticles with a monoclinic structure were formed by using a colloid-thermal synthesis process. D. I. Son, C. H. You and T.W. Kim [76] proposed that CuO nanoparticles were formed in a DMF solution. The optical band-gap energy of CuO nanoparticles at 300 K, as determined

from the absorbance spectrum was 3.63 eV, resulting from the decrease in the dimension of the CuO nanoparticles. X-ray photoelectron spectroscopy profiles showed that the O_{1s} and the Cu_{2p} peaks corresponding to the CuO nanoparticles were observed.

2.2.3 Characterization

2.2.3.1 XRD (x-ray diffraction)

X-ray scattering techniques are a family of non-destructive analytical technique which reveals information about the crystallographic structure, chemical composition, and physical properties of materials and thin films. Powder diffraction (XRD) is a technique used to characterize the crystallographic structure, crystalline size (grain size), and preferred orientation in polycrystalline or powdered solid samples. Powder diffraction is commonly used to identify unknown substances, by comparing diffraction data against a database maintained by the international Centre for Diffraction Data. It may also be used to characterize heterogeneous solid mixtures to determine relative abundance of crystalline compounds, and when coupled with lattice refinement technique, such as Rietveld refinement can provide structural information on unknown materials.

XRD technique determines the crystal structure and composition of the specimens with graphite monochromatized Cukα (1.54056 A°). X-ray generator under ambient conditions. The accelerating voltage was set 50 kV, with 100 mA fluxes at a scanning rate of 0.06/s in the range 5°-80°. The XRD pattern indicate the CuO nanoparticles are single crystalline where the (110) K_{α_1} diffraction peak at 32.65°.

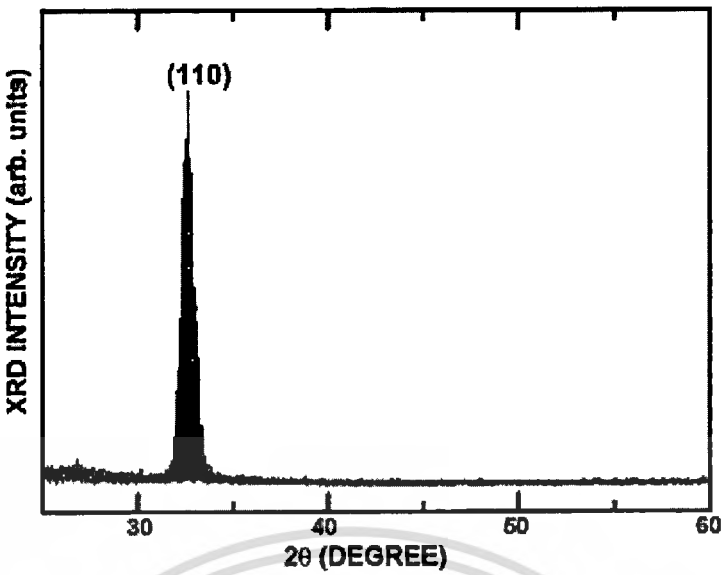

Figure 2.7 XRD pattern of Copper oxide [76]

Powder diffraction is also common method for determining strains in crystalline materials. An effect of the finite crystallite size is seen as a broadening of the peaks which is more meaningful for the calculation of particle size therefore size of nanocrystals has been calculated using Debye-scherer formula using reflection from the XRD pattern. Debye-Scherer formula for crystalline size determination is given by Kuldeep S. et al. [77];

$$D = \frac{0.90\lambda}{\beta\cos\theta}$$

Where D is the crystalline size, λ is the wavelength of x-ray, β is the full width at half maximum (FWHM) after correcting the instrument peak broadening (expressed in radians), θ is the Bragg's angle. The value of particle size obtained from XRD for different molar concentrations.

One type of XRD machine is the Philips Diffractometer, a beam consists of Cu K_{a1} and K_{a2} radiation. The primary facility for this an automated powder diffractometer attached to a 2000 watt examine minute crystals or crystal fragments.

Figure 2.8 XRD machine [78]

X-ray diffraction is a tool for the investigation of the structure of matter. X-ray are scattered by interaction with the electron of the atoms in the material being investigated. The crystal structure is the most fundamental characteristic of crystalline matter. The technique began when von Laue discovered that crystals diffract x-rays in 1912. Since then it has been applied to chemical analysis, stress and strain measurement, and the study of phase equilibrium, measurement of particle size, as well as crystal structure.

2.2.3.2 TEM (transmission electron microscopy)

Transmission electron microscopy (TEM) is a microscopy technique whereby a beam of electron is transmitted through an ultra thin specimen, interaction with the specimen as it passes through. An image is formed from the interaction of the electrons transmitted through the specimen; the image is magnified and focused onto an imaging device, such as a fluorescent screen, on a layer of photographic film, or to be detected by sensor such as a CCD camera.

TEM measures the size distribution [62], average diameter [79], and morphology [62] of the CuO grain. It shows the crystalline [76], shape, and the lattice fringes can be seen by using HRTEM images [72], also can be observed the agglomeration of particle.

Figure 2.9 TEM of CuO nanoparticles (QinetiQ Nanomaterials Ltd) [80]

Sample preparation in TEM can be a complex procedure. TEM specimens are required to be at most hundreds of nanometers thick, as unlike neutron or x-ray radiation the electron beam interact readily with the sample an effect that increases roughly with atomic number squared [57]. High quality sample will have a thickness that is comparable to the mean free path of the electrons that travel through the samples, which may be only a few tens of nanometers.

There are a number of drawbacks to the TEM technique. Many materials require extensive sample preparation to produce a sample thin enough to be electron transparent, which makes TEM analysis a relatively time consuming process with a low throughput of samples. Being almost transparent to electrons, a grapheme substrate has been able to show single hydrogen atom and hydrocarbons. The structure of the sample may also be changed during the preparation process. Also the field of view is relatively small, raising the possibility that the region analyzed may not be characteristic of the whole sample. There is potential that the sample may be damaged by the electron beam, particularly in the case of biological materials.

One type of TEM machine is the JEM-2010 (JEOL) is a high performance transmission electron microscope. The basic instrument is expanded with two additional extensions namely a scanning attachment and an energy dispersive x-ray spectrometer, thus enabling the operator to perform a wide range of measurements.

Figure 2.10 TEM machine [81]

2.2.3.3 FTIR (Fourier transform infrared spectroscopy)

Fourier transform infrared spectroscopy (FTIR) is a technique which is used to obtain an infrared spectrum of absorption, emission, photoconductivity or Raman scattering of a solid, liquid or gas. An FTIR spectrometer simultaneously collects spectral data in a wide spectral range. This confers a significant advantage over a dispersive spectrometer which measures intensity over a narrow range of wavelengths at a time. FTIR has made dispersive infrared spectrometers all but obsolete (except sometimes in the near infrared), opening up new applications of infrared spectroscopy.

The Sample Analysis Process

1. The Source: Infrared energy is emitted from a glowing black-body source. This beam passes through an aperture which controls the amount of energy presented to the sample (and, ultimately, to the detector).

2. The Interferometer: The beam enters the interferometer where the "spectral encoding" takes place. The resulting interferogram signal then exits the interferometer.

3. The Sample: The beam enters the sample compartment where it is transmitted through or reflected off of the surface of the sample, depending on the type of analysis being accomplished. This is where specific frequencies of energy, which are uniquely characteristic of the sample, are absorbed.

4. The Detector: The beam finally passes to the detector for final measurement. The detectors used are specially designed to measure the special interferogram signal.

5. The Computer: The measured signal is digitized and sent to the computer where the Fourier transformation takes place. The final infrared spectrum is then presented to the user for interpretation and any further manipulation.

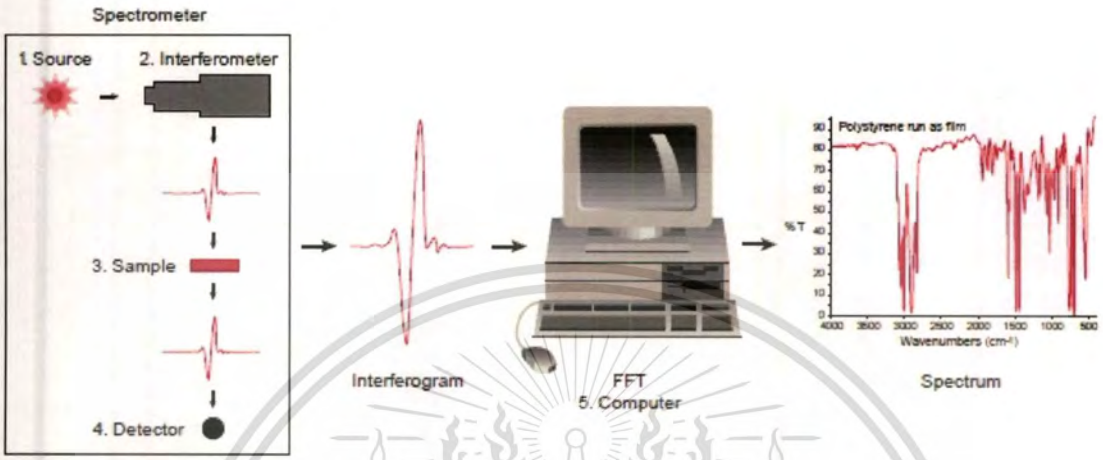

Figure 2.11 the Sample Analysis Process [82]

Figure 2.12 FTIR machine [83]

Because there needs to be a relative scale for the absorption intensity, a background spectrum must also be measured. This is normally a measurement with no sample in the beam. This can be compared to the measurement with the sample in the beam to determine the "percent transmittance."

This technique results in a spectrum which has all of the instrumental characteristics removed. Thus, all spectral features which are present are strictly due to the sample. A single background measurement can be used for many sample measurements because this spectrum is characteristic of the instrument itself.

Some of the major advantages of FTIR over the dispersive technique include:

• **Speed:** Because all of the frequencies are measured simultaneously, most measurements by FTIR are made in a matter of seconds rather than several minutes. This is sometimes referred to as the Felgett Advantage.

• **Sensitivity:** Sensitivity is dramatically improved with FTIR for many reasons. The detectors employed are much more sensitive, the optical throughput is much higher which results in much lower noise levels, and the fast scans enable the condition of several scans in order to reduce the random measurement noise to any desired level

• **Mechanical Simplicity:** The moving mirror in the interferometer is the only continuously moving part in the instrument. Thus, there is very little possibility of mechanical breakdown.

• **Internally Calibrated:** These instruments employ a HeNe laser as an internal wavelength calibration standard. These instruments are self-calibrating and never need to be calibrated by the user.

These advantages, along with several others, make measurements made by FTIR extremely accurate and reproducible. Thus, it a very reliable technique for positive identification of virtually any sample. The sensitivity benefits enable identification of even the smallest of contaminants. This makes FTIR an invaluable tool for quality control or quality assurance applications whether it is batch-to-batch comparisons to quality standards or analysis of an unknown contaminant. In addition, the sensitivity and accuracy of FTIR detectors, along with a wide variety of software algorithms, have dramatically increased the practical use of infrared for quantitative analysis. Quantitative methods can be easily developed and calibrated and can be incorporated into simple procedures for routine analysis.

Thus, the Fourier Transform Infrared (FTIR) technique has brought significant practical advantages to infrared spectroscopy. It has made possible the development of many new sampling techniques which were designed to tackle challenging problems which were impossible by older technology. It has made the use of infrared analysis virtually limitless.

2.2.3.4 SEM (Scanning electron microscopy)

A finely focused electron beam scanned across the surface of the sample generates secondary electrons, backscattered electrons, and characteristic x-rays. These signals are collected by detectors to form image of the sample displayed on a cathode ray tube screen. Features seen the SEM image may then be immediately analyzed for elemental composition using EDS or WDS.

Secondary Electron Imaging shows the topography of surface features a few nm across. Films and stains as thin as 20 nm produce adequate contrast images. Materials are viewed at useful magnifications up to 100,000x without the need for extensive sample preparation and without damaging the sample. Even higher magnifications and resolution are routinely obtained by our Field Emission SEM.

Backscattered Electron Imaging shows the spatial distribution of elements or compounds within the top micron of the sample. Features as small as 10 nm are resolved and composition variations of as little as 0.2% determined.

Data Output is generated in real time on the CRT monitor. Images and spectra can be printed here, recorded on CD-ROM and/or emailed for insertion into your own reports.

Figure 2.13 SEM machine [84]

All samples must also be of an appropriate size to fit in the specimen chamber and are generally mounted rigidly on a specimen holder called a specimen stub. Several models of SEM can examine any part of a 6-inch (15 cm) semiconductor wafer, and some can tilt an object of that size to 45°. For conventional imaging in the SEM, specimens must be electrically conductive, at least at the surface, and electrically grounded to prevent the accumulation of electrostatic charge at the surface. Metal objects require little special preparation for SEM except for cleaning and mounting on a specimen stub. Nonconductive specimens tend to charge when scanned by the electron beam, and especially in secondary electron imaging mode, this causes scanning faults and other image artifacts. They are therefore usually coated with an ultrathin coating of electrically-conducting material, commonly gold, deposited on the sample either by low vacuum sputter coating or by high vacuum evaporation. Conductive materials in current use for specimen coating include gold, gold/palladium alloy, platinum, osmium, iridium, tungsten, chromium and graphite.

2.3 Copper Compound

There are two compounds that we used as a reactant in solid-solid reaction method. For synthesize copper (II) oxide there are $Cu(NO_3)_2$ and $Cu(CH_3COO)_2$.

2.3.1 Preparation

2.3.1.1 Copper nitric

$Cu + 4\ HNO_3 \longrightarrow Cu(NO_3)_2 + 2\ H_2O + 2\ NO_2$ Copper nitric is simple reaction for prepared. The synthesize can be use the copper powders mix with nitric acid in mole ratio 1:4 (Cu: nitric acid) the reaction is extreme exothermic and generate nitrous gaseous so that the reaction very jeopardy.

2.3.1.2 Copper acetate

According to the nitric reaction the nitrous is toxic gas. We will find the new copper compounds with environmentally friendly that is copper acetate the reaction is

$$Cu + H_2O_2 + 2CH_3COOH \longrightarrow Cu(CH_3COO)_2 + 2H_2O$$

The reaction is mild condition and can produce the copper acetate in high volume.

Chapter 3

Experimental Details

The objective of this part of the study was to preparation of the copper (II) oxide nanoparticles by using solid-solid reaction and solid-liquid reaction methods. The effects of the nature and stoichiometric ratio of reactants on the particle morphology of the product were investigated. The products were characterized using XRD, XRF, SEM and TEM respectively.

3.1 Chemicals

1. Cu (powder) by Höganäs
2. Nitric acid (HNO_3) by UNIVAR
3. Acetic acid (CH_3COOH) by QRëC™
4. Hydrogen peroxide (H_2O_2) by CARLO ERBA
5. Sodium hydroxide anhydrous pellet (NaOH) by CARLO ERBA
6. Distilled water
7. Ethanol 95%

3.2 Instruments

1. Mortar and pestle
2. Glassware and Watch glass (container and cover)
3. Ultrasonic wave washer
4. Vacuum filter set
5. X-ray diffractometer, XRD
6. Transmission electron microscope, TEM
7. Scanning electron microscope, SEM
8. Fourier transform infared spectroscopy, FTIR

3.3 Preparation of Copper nitrate

The copper nitrate was prepared by using copper powders reacted with 70% concentration of nitric acid. Afterward evaporate water out at room temperature until to be solid state. The diagram of copper nitrate preparation was shown as below

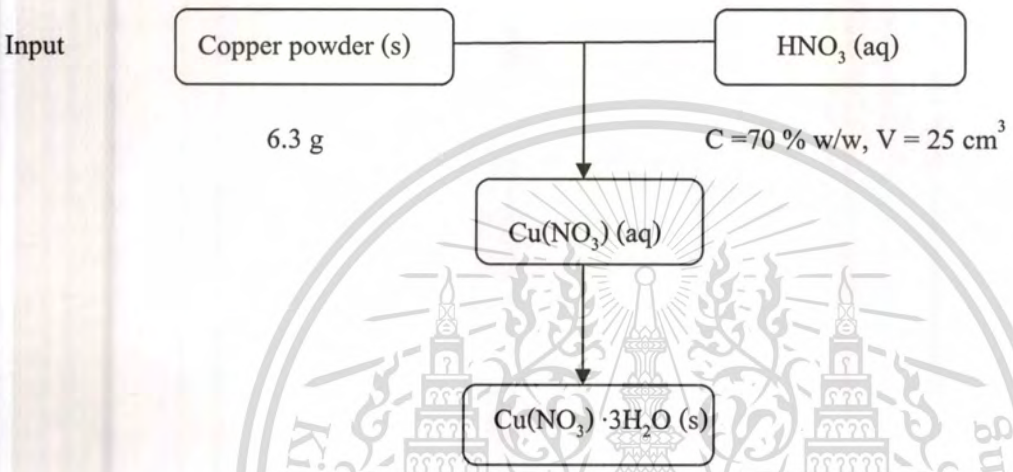

Figure 3.1 Preparation of Copper nitric from copper powders

3.4 Preparation of Copper acetate

The copper acetate was prepared by using glacial acetic acid diluted with H_2O_2 and heats it up until boil. Afterward bring it mixed with copper powders. It will be shown blue-green color. Solution and evaporate water out at room temperature until to be solid state. The diagram of copper acetate preparation was shown below

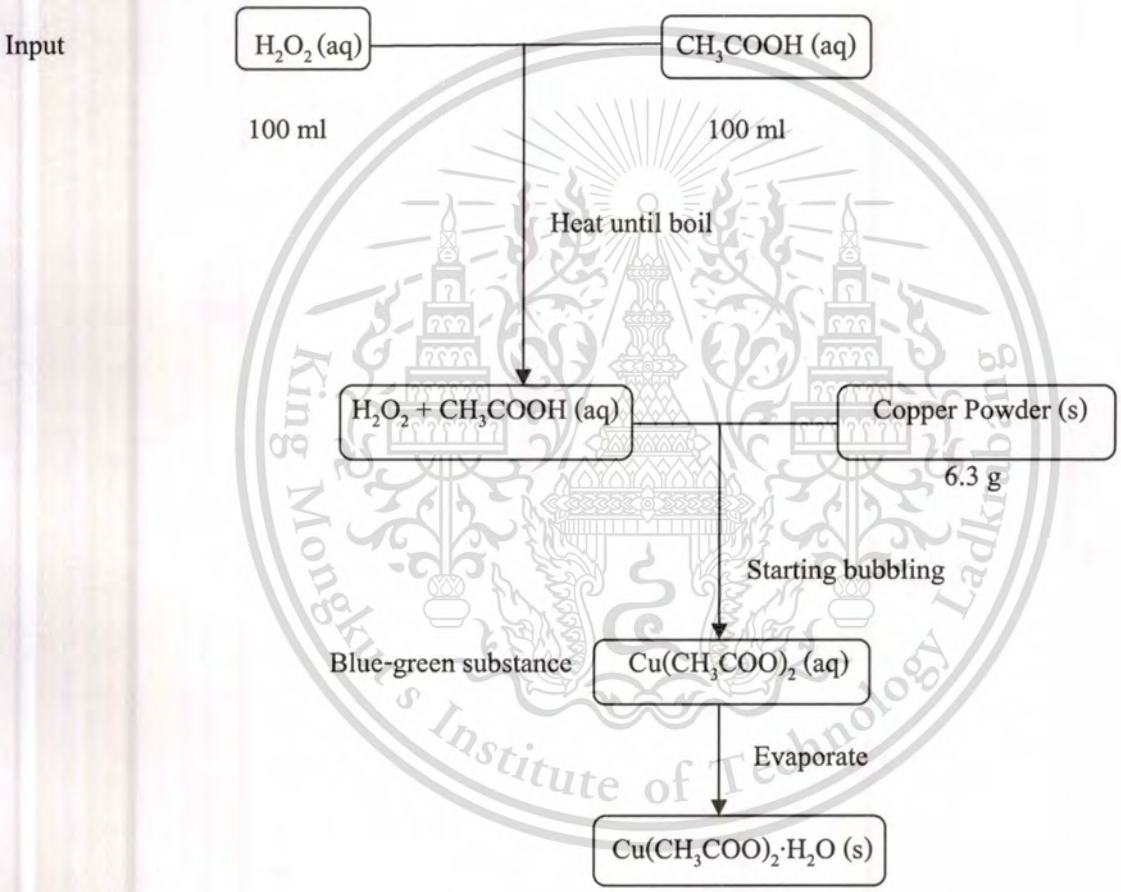

Figure 3.2 Preparation of Copper acetate from copper powders

3.5 Preparation of CuO nanoparticles using solid-solid reaction.

The Copper (II) oxide nanoparticles were prepared by using the solid-solid reaction. The effect of type of copper compounds and hydroxyl alkaline, the molar ratio, particle size distribution and time were studied. The diagram of copper oxide preparation was shown as below.

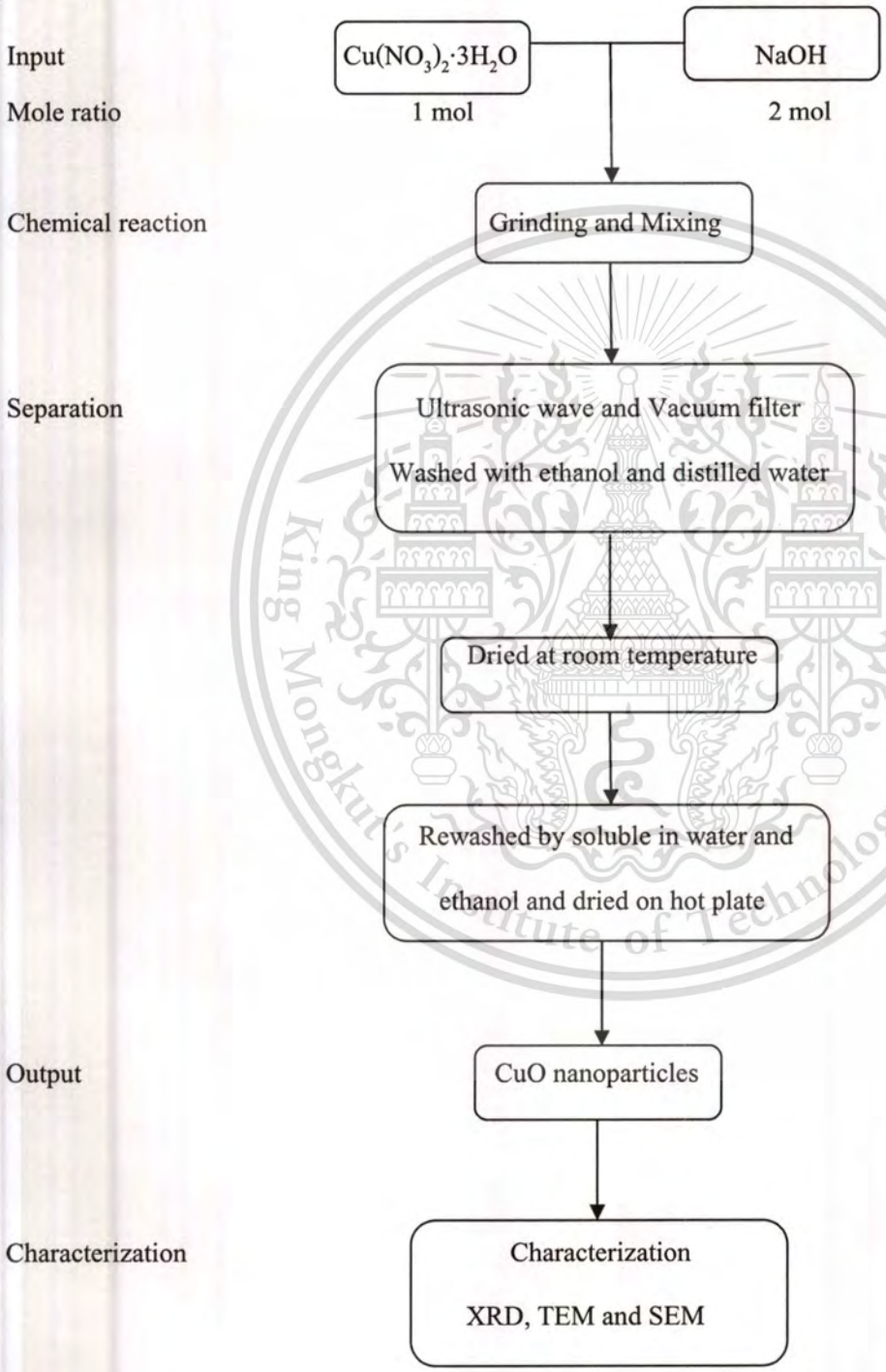

Figure 3.3 Preparation of Copper (II) oxide Nanoparticle by copper nitric

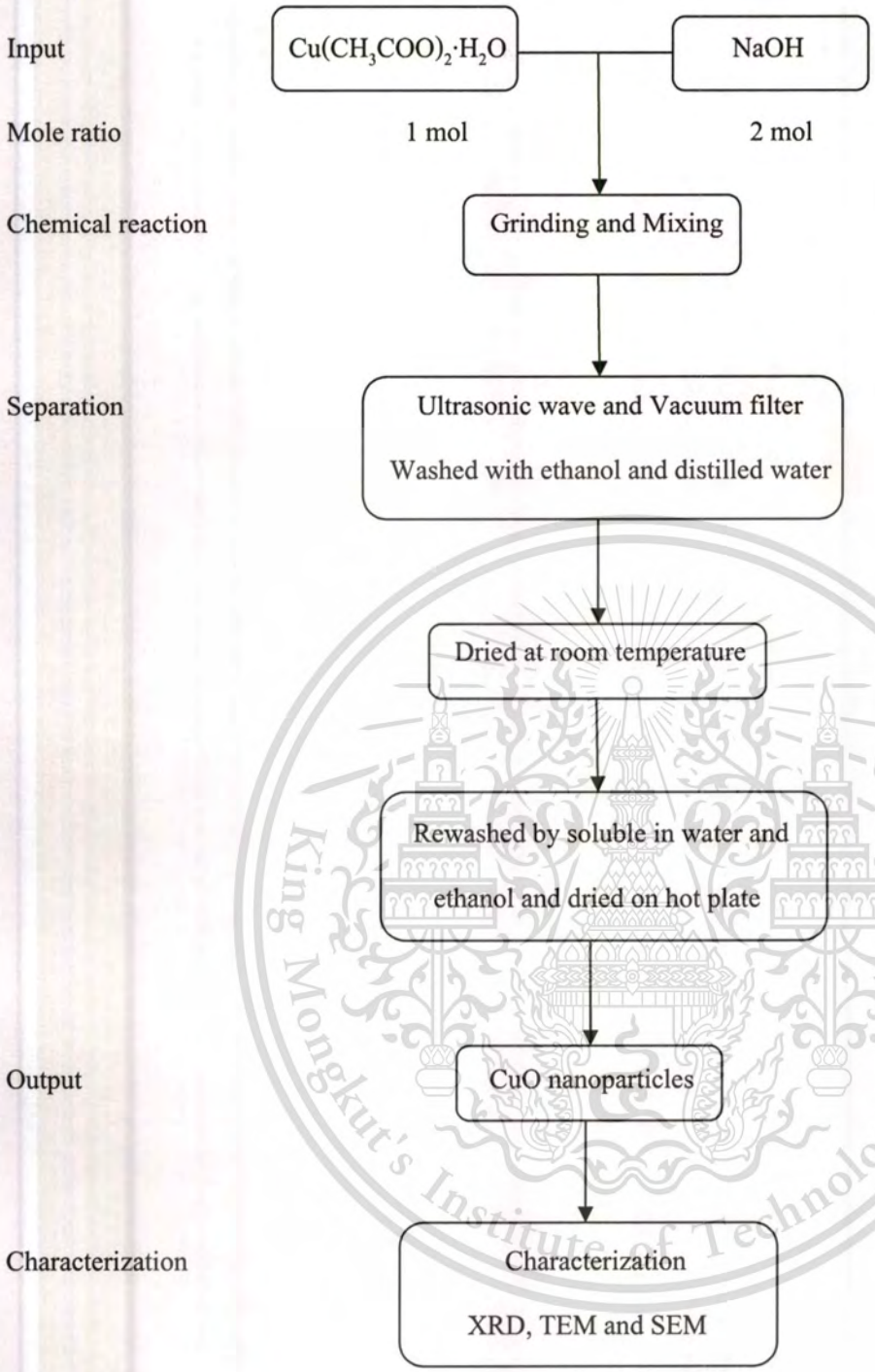

Figure 3.4 Preparation of Copper (II) oxide Nanoparticle by copper acetate

3.5.1 Product Purification

The products were mixed and grinded for 30 minutes, the system was washed with distillated water in an ultrasonic wave washer for 25 minutes. This was then washed in the vacuum filter, three times with distilled water then followed washed by twice with ethanol to remove any remaining unwanted ion. After that the obtain products were died in oven at 60°C for a day.

The further purification the product with water and ethanol in ultrasonic bath and allowed the particle to precipitate for a day. The product were removed and dried on hot plate. This powder was ready for particle characterization.

The XRD was proved to determine the relationship between purity and the washing method.

3.5.2 Yield and Theoretical

The yield of copper (II) oxide nanoparticles were calculated based on the mole balance equation. The following equation describes the nucleation and growth mechanism used to predict the copper (II) oxide obtained.

$$Cu + 4HNO_3 \longrightarrow Cu(NO_3)_2 + 2H_2O + 2NO_2 \quad (3.1) \text{ [exothermic rxn]}$$

$$Cu(NO_3)_2\,(s) + 2NaOH\,(s) \longrightarrow Cu(OH)_2 + NaNO_3 \quad (3.2) \text{ [exothermic rxn]}$$

$$Cu + 2CH_3COOH + H_2O_2 \longrightarrow Cu(CH_3COO)_2 + H_2O \quad (3.3) \text{ [exothermic rxn]}$$

$$Cu(CH_3COO)_2\,(s) + 2NaOH\,(s) \longrightarrow Cu(OH)_2 + 2CH_3COONa \quad (3.4) \text{ [exothermic rxn]}$$

Exothermal step

$$Cu(OH)_2 \longrightarrow CuO + H_20 \quad (3.5)$$

All above equation showed two steps of reaction that a mole of copper compound reactant gave a mole of copper (II) oxide product. For the purpose of this study it was assumed that the reaction has occurred to completion.

Theoretical yield (g) = Mole of copper compound used x Molecular weight of copper oxide

Where; Molecular weight of CuO = 79.55 g/mol

The percent yield is calculated as follow

$$\% \text{ yield} = \frac{\text{actual yield}}{\text{theoretical yield}} \times 100$$

3.6 Characterization of Particles

The objective of this part of the experimental was to determine as effective method to measure the size of the particles prepared and to obtain a clear image of the shape of particles. The following equipments were used to study the particles size during the test work

3.6.1 XRD study

J.F. Xu et al. reported that XRD pattern is identical to pure CuO, without signals from reactant, indicating the formation of monoclinic structure. The XRD study was to determine if this applicable for others copper compound and hydroxyl alkaline.

The sample was washed with water and ethanol to remove any unwanted sodium hydroxide and other precursor ion. This was then precipitated and died on a hot plate to form a black powder. The samples were placed on specimen holder and analyzed using x-ray diffraction. The experimentally identified and catalogued for the CuO nanoparticles with lattice constant match well with the standard diffraction data (JCPDS). A step size of 0.02° of 2theta was taken at 0.02° 2theta / second at 30° to 65°.

3.6.2 TEM study

The transmission electron microscope used was model JEM-2010 by JEOL. The images were used to measure the size of particle and the average was taken as the particle size.

J.F. Xuv et al. reported that copper oxide nanoparticles when prepared with copper chloride and sodium hydroxide, displayed polyhedral nanocrystals. The TEM study was to determine if this applicable for other copper compound and hydroxyl alkaline. CuO particles were prepared at 60°C.

3.6.3 SEM study

SEM was used to analyze the morphology of specimen in high magnification. The images were used to to examine the surface of CuO particles. BSE was used to examine the composition on specimen.

3.7 Effect of Reactant study

There were various parameters that affect the size and crystallinity of particles. The particle size was measured using a transmission electron microscope. The crystallinity was measured using an x-ray diffraction.

The following conditions were studied the $Cu(NO_3)_2 \cdot 3H_20$ and $Cu(CH_3COO)_2$ were prepared from copper powders that were used as copper compound and the NaOH was used as a hydroxyl alkaline in this experiment. The procedure was carried out following the preparation step as in diagram.

Chapter 4

Result and Discussion

4.1 Synthesis route characters

Simplicity of synthesis routes for CuO nanoparticles is important and interested by industrial sectors. The process simplicity may be determined from raw materials types and availability, processing step ease and numbers, environmental friendliness and product yield. The synthesis routes employed in this research (Equations (1) to (4)) seem to be simple for chemists. However, the synthesis route via $Cu(NO_3)_2$ intermediate (Equations (1) and (2)) produces a toxic NO_2 gas. The synthesis route via $Cu(CH_3COO)_2$ intermediate (Equations (3) and (4)), in contrast, seems to be more environmental friendly. When the product yield is concerned, the $Cu(NO_3)_2$ intermediate route produces slightly higher yield than the $Cu(CH_3COO)_2$ intermediate route, as given in Table 4.1, It must be noted here that the synthesized products are nanoparticles (see TEM micrographs in the section 4.4) so loss of some products at each processing step cannot be avoided. Other reasons for yield loss are impurities and some non-dissolved amounts related to the Cu powders raw materials.

Table 4.1 Product yields of the synthesis routes for CuO nanoparticles

Reaction	% yield
$Cu(NO_3)_2$ intermediate (Equations (1) and (2))	72.57
$Cu(CH_3COO)_2$ intermediate (Equations (3) and (4))	70.06

4.2 Characterization of synthesized intermediates

Although the intermediate chemicals (the synthesized $Cu(NO_3)_2$ and $Cu(CH_3COO)_2$) were purified and then dried for several hours, adsorption of humidity on the materials could not be avoided during handling of them before XRD and FTIR tests. The hydrate forms of them were thus obtained. To ensure that two intermediates, namely $Cu(NO_3)_2$ and $Cu(CH_3COO)_2$ existed in the reactions, the ground particles of intermediates were characterized by XRD and FTIR. Figure 4.2.1 shows XRD peaks of the chemical obtained from the reaction between Cu powders and HNO_3 acid. Indexing of some dominant peaks, using JCPDS Card No. 04-013-2990, indicated that the chemical characterized was $Cu(NO_3)_2 \cdot 3H_2O$. The chemical obtained from the reaction between Cu powders and CH_3COOH showed XRD peaks as given in Figure 4.2.2 Indexing of the XRD pattern, by using JCPDS Card No. 46-0859, indicated that the chemical was corresponding to $Cu(CH_3COO)_2 \cdot H_2O$.

Characterization using FTIR technique yielded spectra of the synthesized chemical obtained from the reaction between Cu powders and HNO_3 acid (Figure 4.2.3) and the synthesized chemical obtained from the reaction between Cu powders and CH_3COOH (Figure 4.2.4). Interpretation of FTIR transmittance peaks (in Figure 4.2.3) resulted that vibrations at 1048.67, 1384.64, 3416.90 cm^{-1} were corresponding to N-O stretching, N=O stretching and O-H stretching, respectively. Comparison of the vibrations given in Figure 4.2.3 (this study) with those of $Co(NO_3)_2 \cdot 6H_2O$ [42, 43] and $Mg(NO_3)_2 \cdot 6H_2O$ is given in Table 4.2. This FTIR information confirms that the product of the reaction between Cu powders and HNO_3 acid is a hydrate form of $Cu(NO_3)_2$. Combination of XRD and FTIR interpretations leads to the conclusion that the analyzed chemical is $Cu(NO_3)_2 \cdot 3H_2O$. Interpretation of FTIR transmittance peaks in Figure 4.2.4 resulted that vibrations at 1354.62, 1421.53, 1444.70, 1602.11, and triple peaks (3271.55, 3374.04 and 3478.01) cm^{-1} were corresponding to symmetric CH_3 bending, antisymmetric CH_3 is bending, symmetric C-O stretching, antisymmetric C-O stretching and O-H stretching, respectively. Comparison of the vibrations given in Figure 4.2.4 (this study) with those of $Cu(CH_3COO)_2 \cdot H_2O$ [89] and $Ca(CH_3COO)_2 \cdot H_2O$ [90] is given in Table 4.3 This FTIR information confirms that the product of the

reaction between Cu powders and CH_3COOH acid is a hydrate form of $Cu(CH_3COO)_2$. Combination of XRD and FTIR interpretations leads to the conclusion that the analyzed chemical is $Cu(CH_3COO)_2 \cdot H_2O$.

Table 4.2 Comparison of functional group vibrations of nitrate hydrate salts due to interactions with the infrared

$Co(NO_3)_2 \cdot 6H_2O$ [86, 87]		$Mg(NO_3)_2 \cdot 6H_2O$ [88]		$Cu(NO_3)_2 \cdot 3H_2O$ (This study)	
Wavenumbers (cm^{-1})	Assignments	Wavenumbers (cm^{-1})	Assignments	Wavenumbers (cm^{-1})	Assignments
664	Symmetric in-plane bending	-	-	-	-
729	Antisymmetric in-plane bending	-	-	-	-
870	Out of plane bending	-	-	-	-
1052	Symmetric stretching	-	-	-	-
1629	Antisymmetric stretching	1629	O-H bending	1621.44	O-H bending
1388	Symmetric stretching	1382.87	NO_3^- anion	1384.64	N=O stretching
-	-	3473.56	O-H stretching	3416.90	O-H stretching

Table 4.3 Comparison of functional group vibrations of acetate hydrate salts due to interactions with the infrared.

Hoganite ($Cu(CH_3COO)_2 \cdot H_2O$) [89]		$Ca(CH_3COO)_2 \cdot H_2O$ [90]		($Cu(CH_3COO)_2 \cdot H_2O$) (This study)	
Wavenumbers (cm^{-1})	Assignments	Wavenumbers (cm^{-1})	Assignments	Wavenumbers (cm^{-1})	Assignments
627	COO rocking	616-623	Out of plane O-C-O stretching	628.40	-
687	OCO deformation	659-672	Symmetric O-C-O twisting and rocking	691.84	-
1354	Symmetric CH_3 rocking	1350	Symmetric CH_3 bending	1354.62	Symmetric CH_3 bending
1418*	COO stretching*	1413	Antisymmetric CH_3 bending	1421.53	Antisymmetric CH_3 bending
1443*	Symmetric CH_3 deformation*	1446	Symmetric C-O stretching	1444.70	Symmetric C-O stretching
1598	Asymmetric COO stretching	1604	Antisymmetric C-O stretching	1602.11	Antisymmetric C-O stretching
3269	O-H stretching	3147	O-H stretching	3271.55	O-H stretching
3368		3385		3374.04	
3471		3519		3478.01	

Note: By checking the paper [91] referred by the authors of the reference No. [89], it was found that the $Ca(CH_3COO)_2 \cdot H_2O$ wavenumber of 1415 cm^{-1} was corresponding to antisymmetric CH_3 bending and the wavenumber of 1454 cm^{-1} was corresponding to symmetric C-O bending.

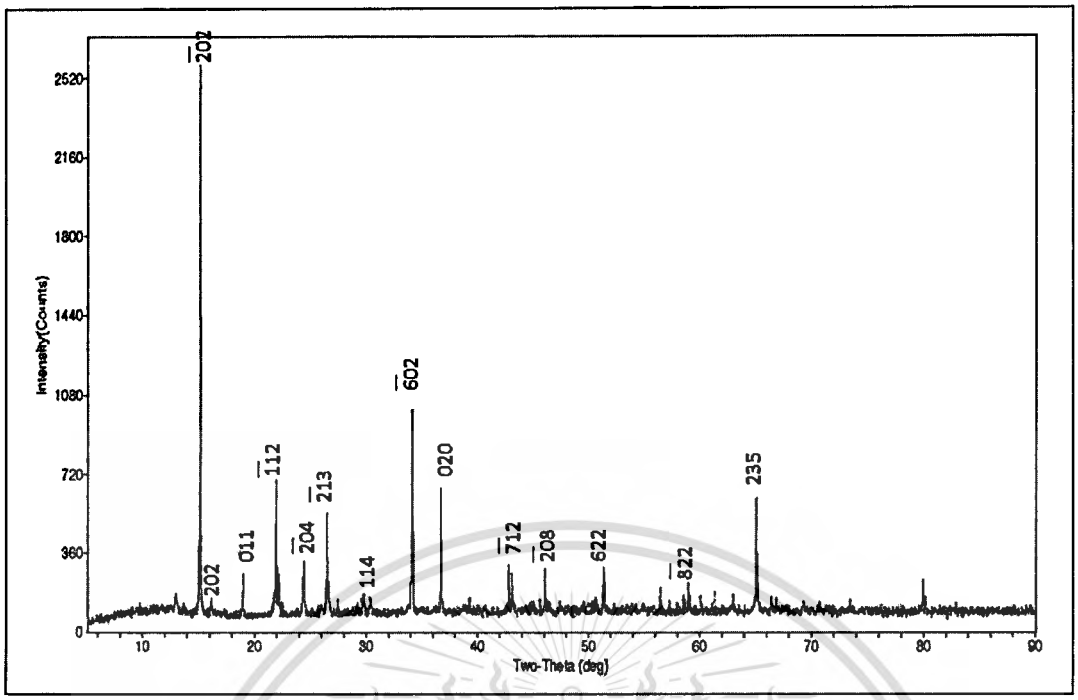

Figure 4.1 XRD pattern of $Cu(NO_3)_2 \cdot 3H_2O$

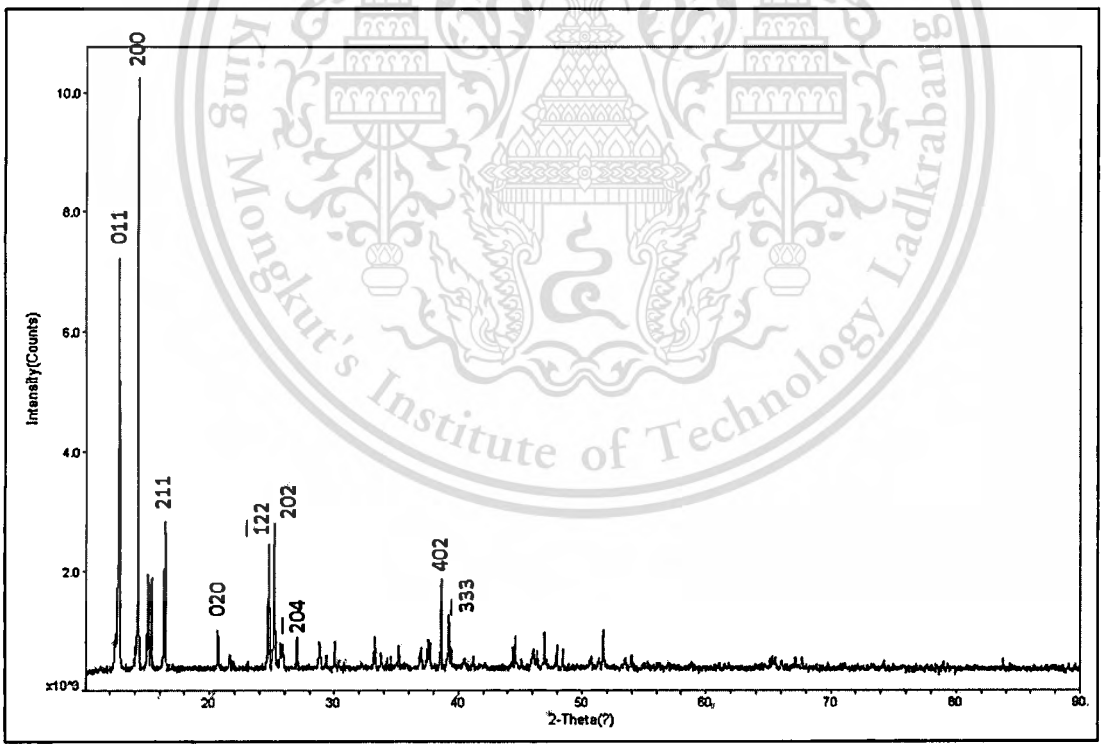

Figure 4.2 XRD pattern of $Cu(CH_3COO)_2 \cdot H_2O$

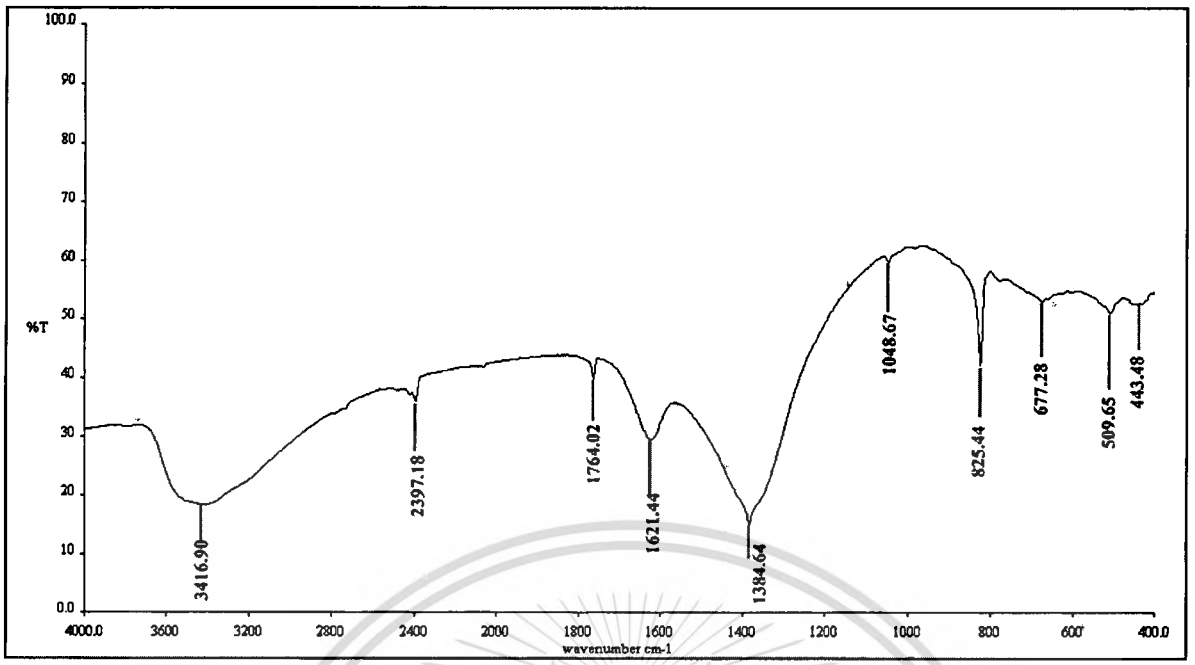

Figure 4.3 FTIR peaks of $Cu(NO_3)_2 \cdot 3H_2O$

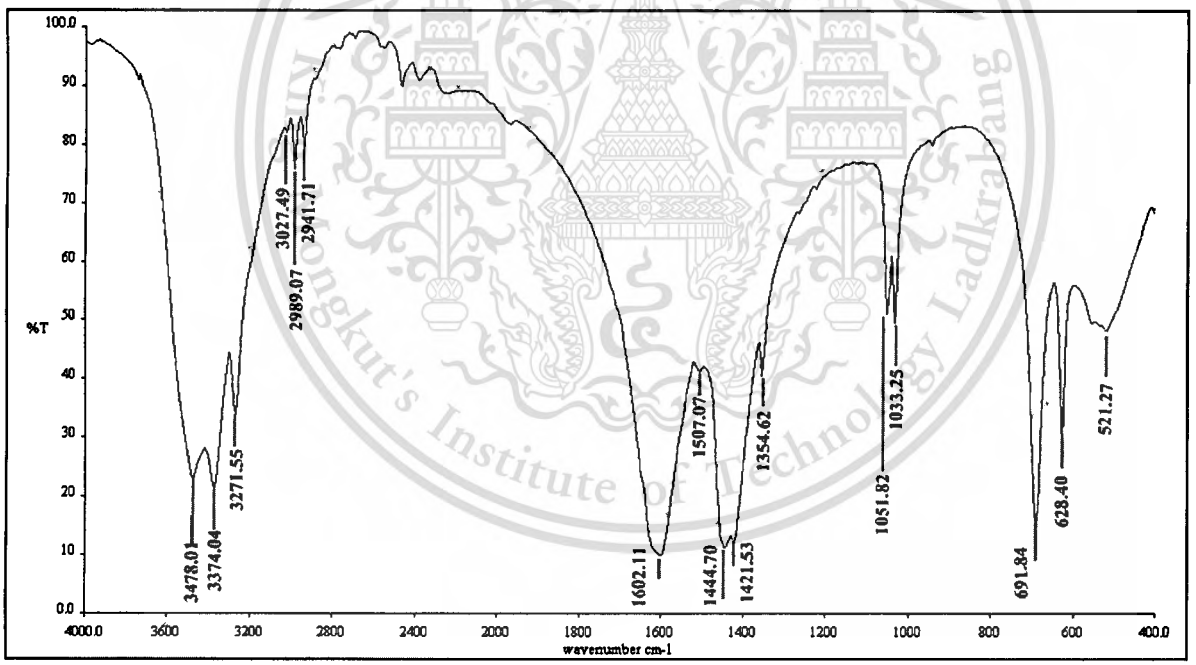

Figure 4.4 FTIR peaks of $Cu(CH_3COO)_2 \cdot H_2O$

4.3 Characterization of CuO nanoparticles by XRD

The synthesized CuO particles from $Cu(NO_3)_2 \cdot 3H_2O$ and $Cu(CH_3COO)_2 \cdot H_2O$ intermediate were characterized by XRD as shown in Figure 4.3.1 and 4.3.2. Both XRD pattern showed broad peaks. Indexing of the XRD peaks by using the JCPDS Card No. 48-1548 of tenorite, it was found that all of the XRD peaks of the synthesized CuO particles were in a good agreement with those of the tenorite. The experimental XRD peaks of the synthesized CuO particles are also in a good agreement with those of CuO nanoparticles synthesized by other routes [3, 4, 7, 9, 11, 25, 37, 40, 42, and 43]. The broad experimental XRD peaks of the synthesized CuO particles are also reassemble to those of CuO nanoparticles synthesized by other routes [3, 7, 37, 42, and 43]. Based on the principle stating that the width of XRD peaks increases as the sizes of the crystalline domains (crystallites) that diffract the x-rays decreases [92-93], broad nature of XRD peaks indicate that the synthesized CuO crystallite sizes lie in the nanometer size. Given in Table 4.4 is the particle measurement by using the Scherrer formula:

$$d = \frac{0.9\lambda}{B\cos\theta} \qquad (5)$$

where d is the average crystallite size, λ is the wavelength of X-ray, B is the full width at the half maximum at diffraction angle θ (in radian). The results of particle measurement by using XRD peak data indicate that the synthesized CuO crystallite sizes are less than 20 nm.

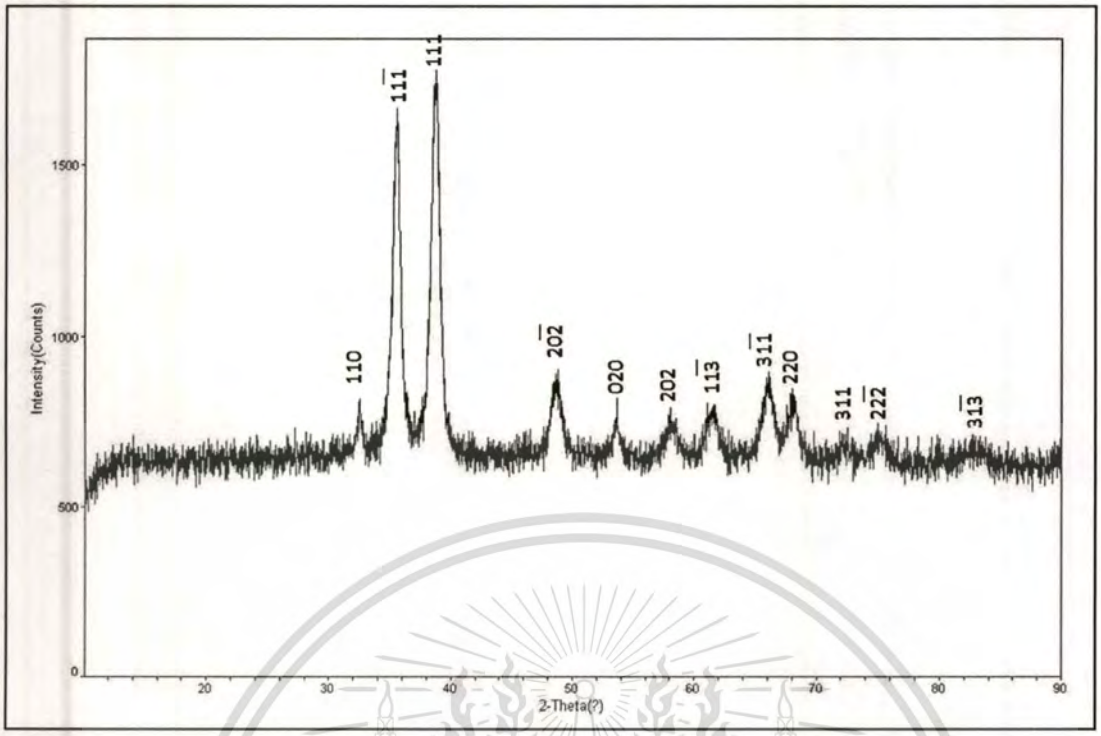

Figure 4.5 XRD pattern of the synthesized CuO nanoparticles from $Cu(NO_3)_2 \cdot 3H_2O$ intermediate.

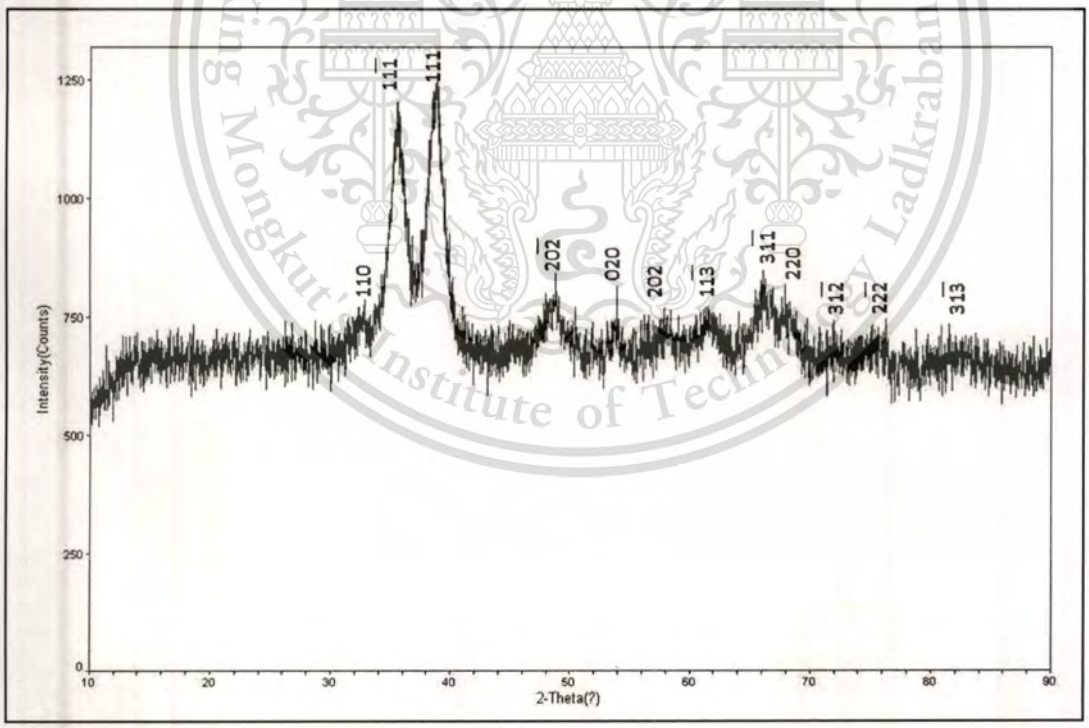

Figure 4.6 XRD pattern of the synthesized CuO nanoparticles from $Cu(CH_3COO)_2 \cdot H_2O$ intermediate.

4.4 Observation of CuO nanoparticles by FE-SEM and TEM

FE-SEM micrographs of the synthesized CuO nanoparticles are shown in Figure 4.4.1. The synthesized CuO nanoparticles from $Cu(NO_3)_2 \cdot 3H_2O$ intermediate exhibited a rod-like form (Figure 4.4.1(b)) whereas the synthesized CuO nanoparticles from $Cu(CH_3COO)_2 \cdot H_2O$ intermediate exhibited a spherical form (Figure 4.4.1(d)). Fine nanoparticle agglomeration resulted in formation of micron-sized porous particles (Figure 4.4.1(a) and (c)). Rough estimation of the particles in Figure 4.3.1(b) and 4.3.1(d) results that the particles have aspect ratio of 10-25 to 25-100 nm and 10 to 10 nm for the synthesized CuO nanoparticles from $Cu(NO_3)_2 \cdot 3H_2O$ and from $Cu(CH_3COO)_2 \cdot H_2O$ intermediates, respectively. This estimation is not accurate due to poor contrast of FE-SEM micrographs.

TEM bright field images and selected area electron diffraction (SAED) patterns of the synthesized CuO nanoparticles from $Cu(NO_3)_2 \cdot 3H_2O$ and $Cu(CH_3COO)_2 \cdot H_2O$ intermediates are shown in Figure 4.4.2. These TEM images not only confirm that the synthesized CuO particles are nanoparticles they also confirm the surface morphology of the synthesized CuO nanoparticle aggregates observed by FE-SEM. The SAED patterns (the insets of Figure 4.4.2) show a ring pattern nature because the selected area is large and it covers a lot of CuO particles. Ring diffraction pattern is generally obtained when the selected area covers polycrystalline region. When the selected area covers a single crystal of CuO nanobelts [40] and CuO nanorods [43, 94], typical electron diffraction spots are obtained. Indexing of the ring SAED patterns (the insets of Fig. 8) is in a good agreement with the interpretation of experimental XRD peaks and SAED pattern indexing of CuO nanowire [4]. Comparison of particle sizes of the synthesized CuO particles measured by using TEM bright field images with those obtained by XRD measurement is given in Table 4.4.

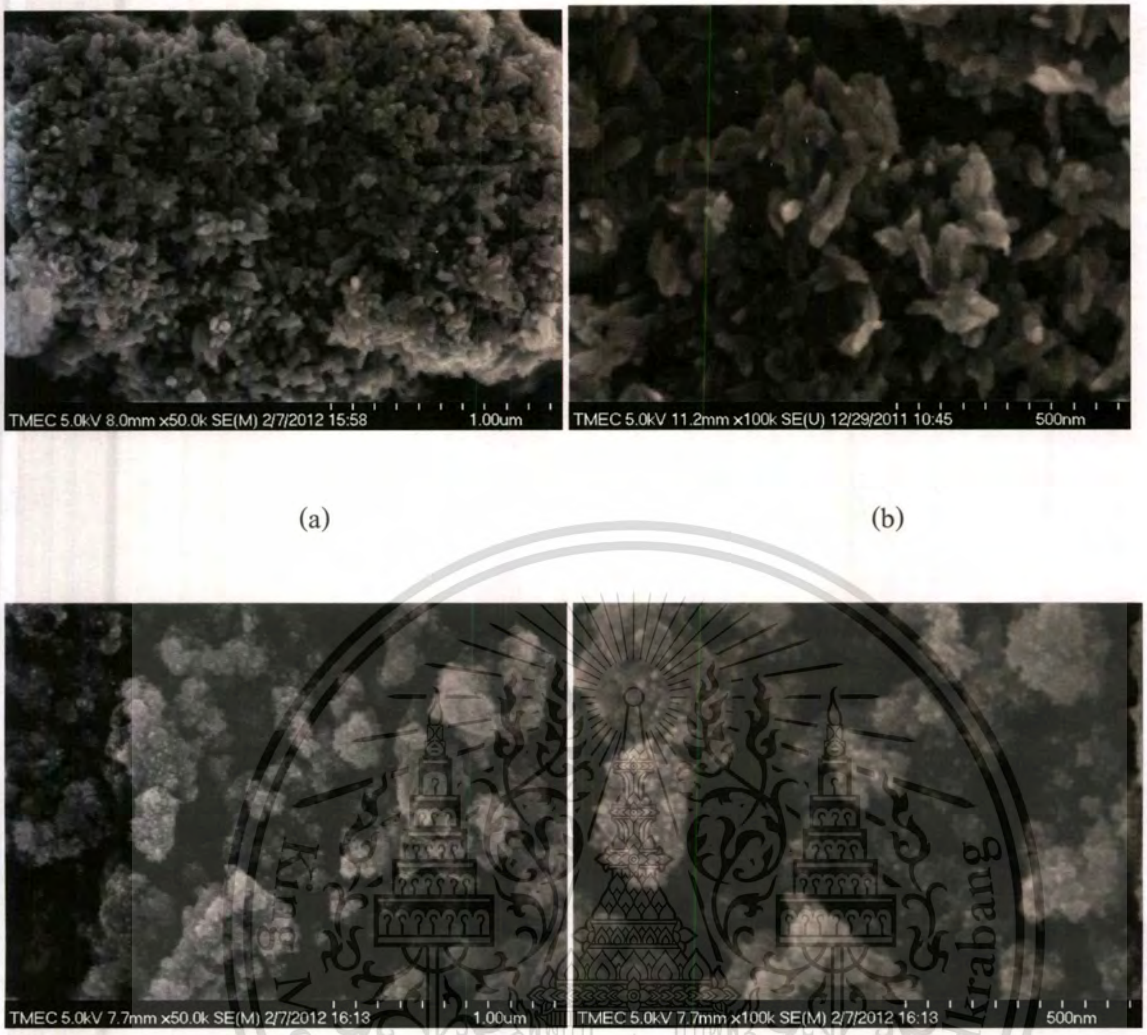

Figure 4.7 SEM micrographs of CuO nanoparticles; (a) and (b) obtained from the reaction between $Cu(NO_3)_2 \cdot 3H_2O$ and NaOH, (c) and (d) obtained from the reaction between $Cu(CH_3COO)_2 \cdot H_2O$ and NaOH

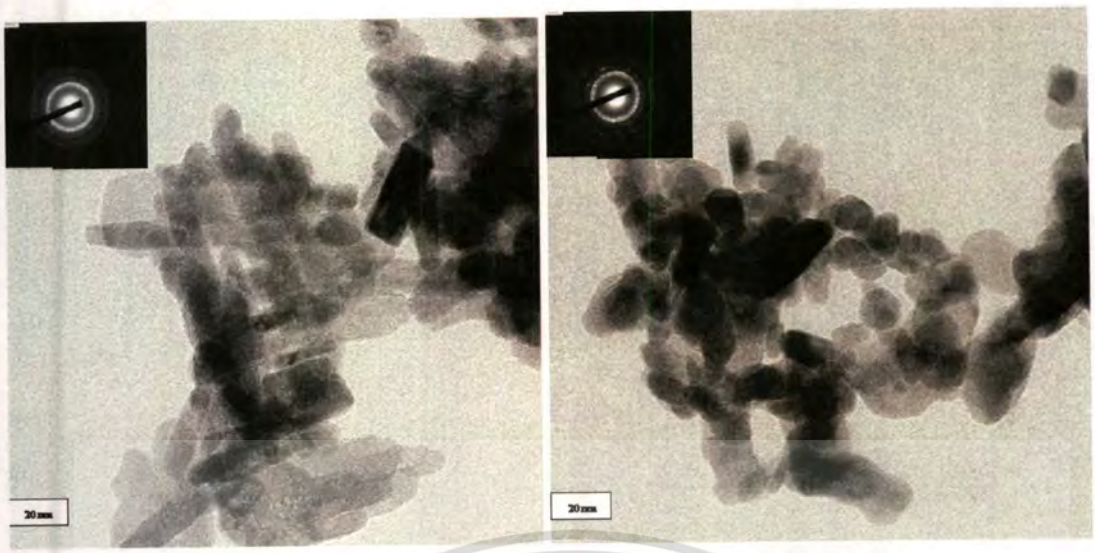

(a)X100,000 (b)X100,000

Figure 4.8 Bright field TEM images and SAED patterns of CuO nanoparticles; (a) obtained from the reaction between $Cu(NO_3)_2 \cdot 3H_2O$ and NaOH and (b) obtained from the reaction between $Cu(CH_3COO)_2 \cdot H_2O$ and NaOH

Table 4.4 CuO particle sizes determined by TEM and XRD

CuO from	Particle size by TEM (nm)		Particle size by XRD (nm)
	Width	Length	
$Cu(NO_3)_2 \cdot 3H_2O$	8.75 ± 1.94	29.29 ± 4.00	14.12 ± 1.83
$Cu(CH_3COO)_2 \cdot H_2O$	10.60 ± 3.15	11.17 ± 1.29	7.59 ± 1.58

4.5 Elemental analysis of the synthesized CuO nanoparticles by SEM-EDS

According to the EDS spectra (Figure 4.5.1), the atomic ratios of the synthesized CuO nanoparticles from the $Cu(NO_3)_2 \cdot 3H_2O$ intermediate was Cu = 65.05% to O = 34.95% and of the synthesized CuO nanoparticles from the $Cu(CH_3COO)_2 \cdot H_2O$ intermediate was Cu = 65.47% to O = 34.53%. These atomic ratios are corresponding to the chemical formula of CuO. Thus the EDS spectra data confirm that the synthesized particles are CuO.

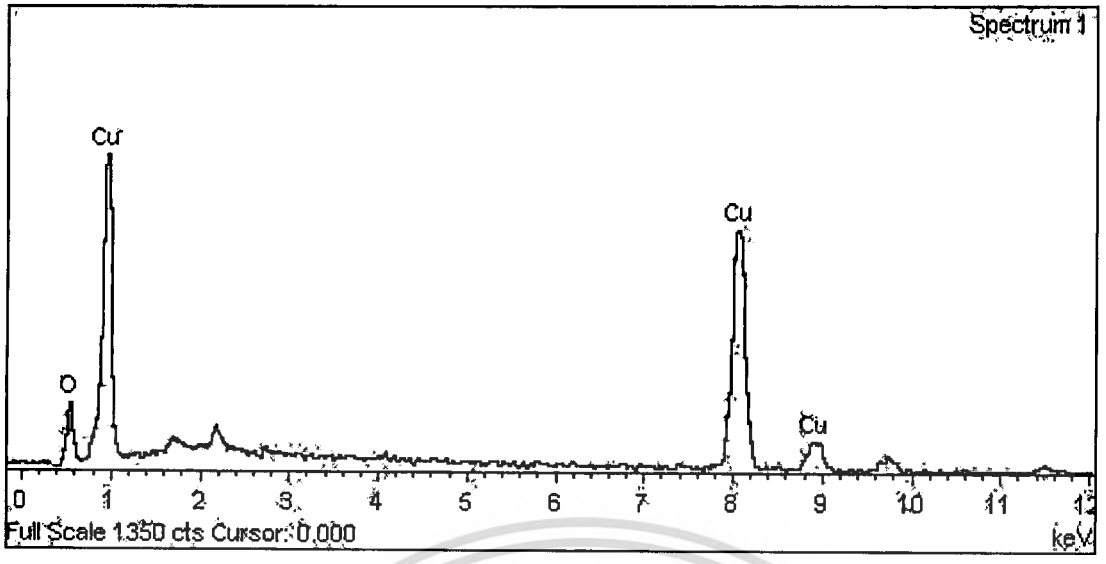

(a)

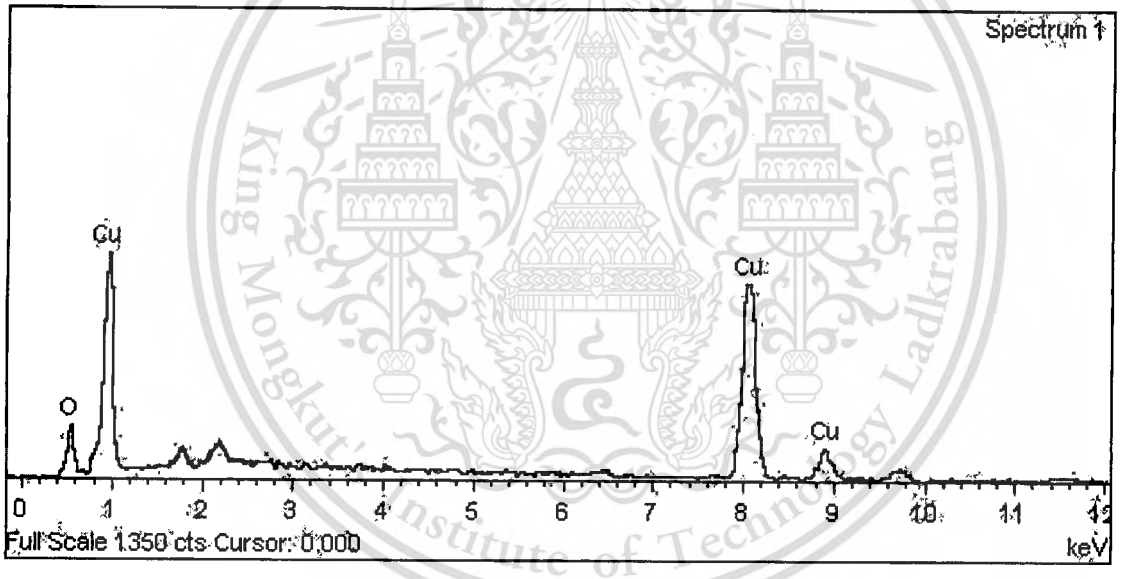

(b)

Figure 4.9 EDS spectra of CuO nanoparticles; (a) obtained from the reaction between $Cu(NO_3)_2 \cdot 3H_2O$ and NaOH and (b) obtained from the reaction between $Cu(CH_3COO)_2 \cdot H_2O$ and NaOH.

Chapter 5

Conclusion and Suggestions

5.1 Conclusion

The simple synthesis routes proposed by us are successful for producing CuO nanoparticles in terms of particle size and yield percentage. Characterizations of chemical intermediates and the products by several techniques including XRD, FTIR, TEM, SEM and EDS all confirm the chemicals related to the proposed synthesis steps given by Equations (1) through (4). The synthesis route via the $Cu(CH_3COO)_2 \cdot H_2O$ intermediate only yield finer CuO nanoparticles it is also an environmental friendly process.

5.2 Suggestion

Further study other strong base such as sodium hydroxide can be used for synthesis copper oxide nanoparticles. The particle size distribution can be change.

Including this research was done with simple laboratory equipments, so that the test of another substance can be found. Test the significance of this experiment must do to compare the performance of the sold copper oxide and synthesis copper oxide.

References

[1] Kummer, J. T. , (1980). Catalysts for automobile emission control, *Prog. Energy Combust. Sci.* 6, 177-199.

[2] Rodriguez, J.A., Kim, J.Y., Hanson J.C., Pérez, M., and Frenkel, A., (2003). Reduction of CuO in H_2: In situ time-resolved XRD studies. *Catal. Lett.* 85, 247-254.

[3] Li, J.-L., Takeguchi, T. and Inui, T., (1996). Doping effect of potassium permanganate on the performance of a copper/zinc oxide/alumina catalyst for methanol formation, *Appl. Catal. A. Gen.,* 139, 97-106.

[4] Pillai, U.R., and Deevi, S., (2006). Room temperature oxidation of carbon monoxide over copper oxide catalyst, *Appl. Catal. B. Env.*, 64, 146-151.

[5] Adam, Y.S., Xu, Z., Fang-ming, J., and Yan, F., (2011). Production of lactic acid from glucose with CuO as a catalyst under hydrothermal conditions, *2011 International Conference on Electrical and Control Engineering (ICECE),* Yichang, China, 16-18 Sept 2011, pp. 4635-4637.

[6] Massa, P.A., Ayude, M.A., Fenoglio, R.J., Gonzalez, J.F., and Haure, P.M., (2004). Catalyst systems for the oxidation of phenol in water, *Latin Amer. Appl. Res.*, 34, 133-140.

[7] Pillai, U.R., and Deevi, S., (2006). Copper-zinc oxide and ceria promoted copper-zinc oxide as highly active catalysts for low temperature oxidation of carbon monoxide, *Appl. Catal., B. Env.* 65, 110-117.

[8] Taylor, S., and Rhodes, C., (2006). The oxidation of carbon monoxide at ambient temperature over mixed copper-silver oxide catalysts, *Catal. Today*, 114, 357-361.

[9] Luo, M.F., Song, Y.P., Lu, J.Q., Wang, X.U., and Pu, Z.Y., (2007). Identification of CuO species in high surface area Cu)-CeO_2 catalysts and their catalytic activities for Co oxidation, *J. Phys. Chem.*, 111, 12686-12692.

[10] Jin, Z.N., and Song, Y.P., (2009). Prepararion of a novel monolithic catalyst CuO-CeO_2 and its catalytic property in VOC oxidation, *Ind. J. Chem.*, 48A, 793-796.

[11] Neiva, L.S., Andrade, H.M.C. and Gama, L., (2011). CuO-CeO_2 catalytic systems destined for CO removal synthesized by means of the Pechini method : An evaluation of the structures obtained, *J. Chem. Eng. Mater. Sci.*, 2(5), 69-75.

[12] Li, L., Zhan, Y., Zheng, Q., Zheng, Y., Chen, C., She, Y., Lin, X., and Wei, K., (2009). Water-gas shift reaction over CuO/CeO_2 catalysts: Effect of thermal stability and oxygen vacancies of CeO2 supports previously prepared by different metods, *Catal. Lett.*, 130, 3-4.

[13] She, Y., Li, L., Zhan, Y., Lin, X., Zheng, Q., and Wei, K., (2009). Effect of yttrium addition on water-gas shift reaction over CuO/CeO_2 catalysts, *J. Rare Earths*, 27(3), 411-417.

[14] Djinovic, P., Batista, J., and Pintar, A., (2008). Calcination temperature and CuO loading dependence on CuO-CeO2 catalyst activity for water gas shift reaction, *Appl. Catal. A. Gen.*, 347, 23-33.

[15] Arai, T., Yanagida, M., Konoshi, Y., Iwasaki, Y., Sugihara, H., and Sayama, K., (2008). Promotion effect of CuO co-catalyst on WO_3-catalyzed photodegradation of organic substances, *Catal. Commun.*, 9, 1254-1258.

[16] Sayama, K., Hayashi, H., Arai, T., Yanagida, Gunji, T., and Sugihara, H., (2010). Highy active WO_3 semiconductor photocatalyst prepared from amorphous peroxo-tungstic acid for the degradation of various organic compounds, *Appl. Catal, B. Env.*, 94, 150-157.

[17] Gines, M.J.L., Marchi, A.J., and Apesteguia, C.R., (1997). Kinetic study of the reverse water-gas shift reaction over CuO/ZnO/Al_2O_3 catalysts, *Appl. Catal. A. Gen.*, 154, 155-171.

[18] Li, Y., Fu, Q., and Flytzani-Stephanopoulos, M., (2000). Low-temperature water-gas shift reaction over Cu- and Ni- loaded cerium oxide catalyst, *Appl. Catal. B. Env.*, 27, 179-191.

[19] Smith, R.J., Loganathan, M., and Shantha, M.S., (2010). A review of water gas shift reaction kinetics, *Int. J. Chem. React. Eng.*, 8, 1-32.

[20] Kim, A.R., Lee, B., Park, M.J., Moon, J.D., and Bae, J.W., (2012). Catalytic performance on CuO/Cr2O3-Ga2O3 mixed oxides for water gas shift reaction : Effect of Gq/Cr molar ratio, *Catal. Commun.*, 19, 66-69.

[21] Vijaikumar, S., Subramanian, T., and Pitchumani, K., (2008). Zeolite encapsulated nanocrystalline CuO : A redox catalyst for the oxidation of secondary alcohols, *J. Nanomater.*, 2008, 1-7.

[22] Nezamzadeh-Ejhieh, A., and Salimi, Z., (2011). Solar photocatalytic degradation of o-phenylenediamine by heterogeneous CuO/X zeorite catalyst, *Desalination*, 280, 281-287.

[23] Gupta, V., Mozumdar, S., Chowdhuri, A., and Sreenivas, K., (2005). *Pramana J. Phys.*, 65(4), 647-652.

[24] Amano, F., Suzuki, S., Yamamoto, T., and Tanaka, T., (2006). *Appl.Catal. B. Env.*, 64, 282-289.

[25] Bakhtiari, F., and Darezereshki, E., (2011). One-step synthesis of tenolite (CuO) nano-particles from $Cu4(SO_4)(OH)_6$ by direct thermal-decomposition method, *Mater. Lett.*, 65, 171-174.

[26] Li, Y., Wei, Y., Shi, G., Xian, Y., and Jin, L., (2011). Facile synthesis of leaf-like CuO nanoparticles and their application on glucose biosensor, *Electroanalysis*, 23(2), 497–502.

[27] Jia, D., Yu, J., and Xia, X., (1988), Synthesis of CuO nanometer powder by one step solid state reaction at room temperature, *Chinese Sci. Bull.*, 43(7), 571-573.

[28] Topnani, N., Kushwaha, S., and Athar, T., (2010). Wet synthesis of copper oxide nanopowder, *Int. J. Green Nanotech. Mater. Sci. Eng.*, 1(2), M67-M73.

[29] Chand, P., Gaur, A., and Kumar, A., (2011). Study of CuO nanoparticles sythesized by sol-gel method, *AIP Conference Proceedings*, 1393(1), 211-212.

[30] Su, Y.K., Shen, C.M., Yang, H.T., Li, H.L., and Gao, H.J., (2007). Controlled synthesis of highly CuO nanowire arrays by template-based sol-gel route, *Trans. Nonferrous Met. Soc. China*, 17, 783-786.

[31] Armelao, L., Barreca, D., Bertapelle, M., Bottaro, G., Sada, C., and Tondello, E., (2002). Sol-gel synthesis and characterization of CuO-based nanosystems, MRS Proceedings 20002, 737-741. (2002 MRS Fall Meeting, December 2-6, 2002, Boston, MA).

[32] Kumar, R.V., Elgamiel, R., Diamant, Y., and Gedanken, A., (2001). Sonochemical preparation and characterization of nanocrystalline copper oxide embedded in poly(vinyl alcohol) and its effect on crystal growth of copper oxide, *Langmuir*, 17, 1406-1410.

[33] Wang, H., Xu, J.Z., Zhu, J.J., and Chen, H.Y., (2002). Preparation of CuO nanoparticles by microwave irradiation, *J. Cryst. Growth*, 244, 88-94.

[34] Guo, L., Tong, F., Liu, H., Yang, H., and Li, J., (2012). Shape-controlled synthesis of self-assembly cubic CuO nanostructures by microwave, *Mater. Lett.*, 71, 32-35.

[35] Martis, P., Venugopal, B.R., Seffer, J.-F., Delhalle, J., and Mekhalif, Z., (2011). Infrared irradiation controlled decoration of multiwalled carbon nanotubes with copper/copper oxide nanocrystals, *Acta Mater.* 59(12), 5040-5047.

[36] Carnes, C.L., Stipp, J., and Klabunde, K.J., (2002). Characterization and adsorption studies of nanocrystalline copper oxide and nickel oxide, *Langmuir*, 18(4), 1352-1359.

[37] Fan, H., Yang, L., Hua., W., Wu, X., Wu, Z., Xie, S., and Zou, B., (2004). Controlled synthesis of monodispersed CuO nanocrystals, *Nanotech.*, 15, 37-42.

[38] Chiang, C.-Y., Aroh, K., and Ehman, S.H., (2012). Copper oxide nanoparticles made by flame spray pyrolysis for photoelectrochemical water splitting-Part I. CuO nanoparticle preparation, *Int. J. Hydrogen Energy*, 37(6), 4871-4879.

[39] Kakihata, T., Usami, K., Yamamoto, H., and Shibata, J., (1998). Preparation of metal oxide powders from metal loaded versatic acid, *Tech. Rep. Kansai Univ.*, 40, 67-79.

[40] Du, G.H., and Van Tendeloo, G., (2004). Cu(OH)2 nanowires, CuO nanowires and CuO nanobelts, *Chem. Phys. Lett.*, 393, 64-69.

[41] Morozov, I.V., Znamenkov, K.O., Korenev, Yu.M., and Shlyakhtin, O.A., (2003). Thermal decomposition of Cu(NO3)2.3H2O at reduced pressures, *Thermochimica Acta*, 403, 173-179.

[42] Lanje, A.S., Shama, S.J., Pode, R.B., and Ningthoujam, R.S., (2010). Synthesis and optical charactertization of copper oxide nanoparticles, *Adv. Appl. Sci. Res.*, 1(2), 36-40.

[43] Wang, L., Zhao, B., Yuan, Z.Y., Zhang, X.J., Wu, Q.D., Chang, L.X., and Cheng, W.J., (2007). Synthesis of CuO nanostructures in ionic liquids, *Sci. China Series B. Chem.*, 50(1), 63-69.

[44] Copper (II) Oxide Available at: URL http://en.wikipeadia.org/wiki/Copper(II)_oxide

[45] Copper Oxide structure, Available at: URL
http://www.webelements.com/compounds/copper/copper_oxide.html

[46] American element. Copper Oxide Nanopowder.

Available at: URL http://www.americanelements.com/cuoxnp.html

[47] A. K. Srivastava, P. Tiwari, A. Kumar, R. V. Nandedkar, Growth of copper oxide nanorods, *Current Science*, Vol. 86, (2004)

[48] A. K. SRIVASTAVA, P.T. ASHWANI KUMAR, R.V. NANDEDKAR, Synchrotron Utilization Division, *Centre for Advanced Technology*, Indore 452 013

[49] Lijuan Chen, Liping Li, Guangsho Li, Synthesis of CuO nanorods and their catalytic activity I the thermal decomposition of ammonium per chlorate, *Journal of alloys and compounds* 464 (2008) 532-536

[50] P.Rak, A.Gar, T.Chai, P.Mang, N.Mang, S.Cho, *Ethanol sensing properties of CuO nanowires prepared by an oxidation reaction*, Ceramics 35 (2009) 649-652

[51]Copper Oxide Powder (CuO and Cu_2O) Available at: URL http://www.reade.com

[52] K. Zhang, C. Rossi, C. Tenailleau, P. Alphonse and J. Chane Ching: *Synthesis of large area and aligned copper oxide nanowires from copper thin film on silicon substrate.*

[53] Xue Wang, Chenguo Hu, Guojun Du, Xiaoshan Ho, Yi Xi, *Synthesis of CuO nanostructures application for non enzymatic glucose sensing, Sensor and actuators* B 144 (2010) 220-225

[54] M. Yang, J. He, Fine tuning of the morphology of copper oxide nanostructures and their application in ambient degradation of methylene blue, *Journal of colloid and interface science* 355 (2011) 15-22

[55] Gao-Qing Yuan, Huan-Feng Jiang, ChangLin, Shi-Jun Liao, Shape and size-controlled electrochemical synthesis of cupric oxide nanocrystal, *Journal of crystal growth* 303 (2007) 400-406

[56] Super conductor, Available at: URL http://www. Science.ca/scientists

[57] D.Chen, G.Shen, K.Tang, Y. Qian, Large-scale synthesis of CuO shuttle-like crystals via a convenient hydrothermal decomposition route, *Crystal Growth* 254 (2003) 225-228

[58] J. Pike, S.W. Chan, F. Zhang, X. Wang, J. Hanson, Formation of stable Cu_2O from reduction of CuO nanoparticles, *Appl. Catal.* A 303 (2006) 273-277

[59] J. Zhu, Dan Li, H. Chen, X. Yang, Lude Lu, X. Wang, Highly dispersed CuO nanoparticles prepared by a novel quick-precipitation method, *Matter. Lett.* 58 (2004) 3324-3327

[60] Z. Hong, Y. Cao, J. Deng, A convenient alcohothermal approach for low temperature synthesis of CuO nanoparticles, *Matter. Lett.* 52 (2002) 34-38

[61] J. Zhu, Dan Li, H. Chen, X. Yang, Lude Lu, X. Wang, Highly dispersed CuO nanoparticles prepared by a novel quick-precipitation method, *Matter. Lett.* 58 (2004) 3324-3327

[62] H. Wang, J.Zh. Xu, J.J.Zhu, H.Y. Chen, Preparation of CuO nanoparticles by microwave irradiation, *Crystal Growth* 244 (2002) 88-94

[63] J. Zhu, H. Chen, H. Liu, X. Yang, L.Lu, X. Wang, Needle-shaped nanocrystalline CuO prepared by liquid hydrolysis of $Cu(OAc)_2$, *Matter. Sci. and Eng* A 384 (2004) 172-176

[64] G.H. Du, G. Van Tendeloo, $Cu(OH)_2$ nanowires, CuO nanowires and CuO nanobelts, *Chem. Phys. Lett.* 393 (2004) 64-69

[65] F.Teng, W.Yao, Y. Zheng, Y.Ma, Y.Teng, T.Xu, S.Liang, Y.Zhu, Synthesis of flower-like CuO nanostructures as a sensitive sensor for catalysis. *Sensors Actuators. Chin.Univ.* B 134 (2008) 761-768

[66] Manmeet Kaur, K.P. Muthe, S.K. Despande, Shipra Choudhury, J.B. Singh, Neetika Verma, S.K. Gupta and J.V. Yakhmi, Growth and branching of CuO nanowires by thermal oxidation of copper, *Journal of Crystal Growth* 289 (2006) 670-675

[67] T. Ahmad a, R. Chopra a, K. V. Rammanujachary b, S. E. Loflandb, A. K. Ganguli, Cantedantiferromahnetism in copper oxide nanoparticles synthesized by the reverse-micellar route, *Solid State Sci.* 7 (2005) 891-895

[68] Lei Sun, Z. Zhang, Z. Wang, Z. Wu, H. Dang, Synthesis and characterization of CuO nanoparticles from ammonia, *Material Research Bulletin* 40 (2005) 1024-1027

[69] M. Guedes, J. M. F. Ferreirab, A. C. Ferro, A study on the aqueous dispersion mechanism of CuO powders using Tiron, *Colloid and Interface Science* 330 (2009) 119-124

[70] S. Wang, H. Xu, L. Qian, Xi Jia, J. Wang, Y. Liu, W. Tang, CTAB assisted synyhesis and photpcatalytic property of CuO hollow microspheres, *Solid State Chem.* 182 (2009) 1088-1093

[71] D. Han, H. Yang,C. Zhu, F. Wang, Controlled synthesis of CuO nanoparticles using TritonX 100 based water in oil reverse micelles, *Powder Technology* 185 (2008) 286-290

[72] Wang Li et al. Syntheses of CuO nanostructures in ionic liquids, Sci China Ser B Chem 50 (2007) 63-69

[73] H. Zhang. J. Feng. M. Zang. Preparation of flower-like CuO by a sinple chemical precipitation method and their application as electrode materials for capacitor, *Material Research Bulletin* 43 (2008) 3211-3226

[74] M.A. Dar, Y.S. Kim, J.M. Sohn, H.S. Shin, Structural and magnetic properties of CuO nanoneedles synthesized by hydrothermal method, *Appl. Surf. Sci.* 254 (2008) 7477-7481

[75] G. Wang, M. Liu, G. Wang, H. Hu, J. Li. K. Liu, X. J. Zhang, B. Fang, Preparation of CuO-Nanoparticle-Modified Electrode and Its Application in the Determination of Rutin, *Anal. Lett*, 1532-236X, (2009) 42-8

[76] D.I. Son, C.H. You, T.W. Kim, Structural, optical and electronic properties of colloidal CuO nanoparticles formed by using a colloid thermal synthesis process, *Appl. Surf. Sci.* 255 (2009) 8794-8797

[77] Kuldeep S. et al, Structural an optical characterization of chemically synthesized ZnS nanoparticles, *Chalcogenide Letter* 5 (2006) 105-110

[78] XRD machine, Available at: URL http://ag.arizona.edu

[79] T. Premkumar, K.E. Geckeler, A green approach to fabricate CuO nanoparticles, *Phys.Chem. Solid* 67 (2006) 1451-1456

[80] R.P. Allaker, J, Dent. Res., 2010, 89(11), 1175-1186

[81] TEM machine, Available at: URL http://www.mae.ntu.edu.eg

[82] Introduction of FTIR, Available at: URL www.thermonicolet.com

[83] FTIR machine, Available at: URL http://maritzapere6270.wordpress.com/

[84] SEM machine, Available at: URL http://www.knowles.com

[85] Morakotjinda, M., Fakpan, K., Yotkaew, T., Tosangthum, N., Krataitong, R., Daraphan, A., Siriphol, P., Wila, P., Vetayanugul, B., and Tongsri, R., (2010). Gas atomization of low melting-point metal powders, *Chiang Mai J. Sci.* 37(1), 55-63, 2010.

[86] Glaspell, G., (2004). Formation and characterization of metal and metal oxide nano particles, Ph.D. Dissertation, The College of Arts and Sciences at West Virginia University, 2004.

[87] Glaspell, G.P., Jagodzinski, P.W., Manivannan, A., (2004). Formation of cobalt nitrate hydrate, cobalt oxide, and cobalt nanoparticles using laser vaporization controlled condensation, *J. Phys. Chem. B.*, 108(28), 9604-9607.

[88] Farooq, M., Ramli, A., Subbarao, D., (2011). The effect of MgO loading on surface properties of γ-Al2O3 in the mixed oxides, *Aus. J. Basic Appl. Sci.*, 5(11), 1342-1351.

[89] Musumeci, A., and Frost, R., (2007). A spectroscopic and thermoanalytical study of the mineral Hoganite, *Spectrochimica Acta Part A.*, 67(1), 48-57.

[90] Musumeci, A., Frost, R., and Waclawik, E.R., (2007). A spectroscopic study of the mineral paceite (calcium acetate), *Spectrochimica Acta Part A,* 67(3-4), 649-661.

[91] Koleva, V., (2005). Vibrational behavior of calcium hydrogen triacetate monohydrate, $CaH(CH_3COO)_3.H_2O$, *Croatica Chemica Acta*, 78(4), 581-591.

[92] Williamson, G.K., and Hall, W.H., (1953). X-ray broadening from filed aluminium and wolfram, *Acta Met.*, 1, 22-31.

[93] Cullity, B.D., (1978). Elements of X-ray diffractions, Addison-Wesley, Reading, MA, pp. 100-103.

[94] Wu, H.Q., Wei, X.W., Shao, M.W., Gu, J.S., and Qu, M.Z., (2002). Synthesis of copper oxide nanoparticles using carbon nanotubes as templates, *Chem. Phys. Lett.*, 364, 152-156.